Short title: Modeling the effects of tDCS in depression

Title: Effects of transcranial direct current stimulation for treating depression: A modeling study

Gábor Csifcsák[1*], Nya Mehnwolo Boayue[1*], Oula Puonti[2,3], Axel Thielscher[2,3], Matthias Mittner[1]

[1]Department of Psychology, UiT The Arctic University of Norway, Tromsø, Norway

[2]Center for Magnetic Resonance, Department of Electrical Engineering, Technical University of Denmark, Kgs Lyngby, Denmark

[3]Danish Research Centre for Magnetic Resonance, Centre for Functional and Diagnostic Imaging and Research, Copenhagen University Hospital Hvidovre, Copenhagen, Denmark

*These authors contributed equally to this work

Corresponding author: Gábor Csifcsák, Department of Psychology, UiT The Arctic University of Norway, Huginbakken 32, 9037 Tromsø, Norway, Phone: +47 77 64 67 76, Fax: +47 77 64 52 91, Email: gabor.csifcsak@uit.no

Word count (Abstract): 239

Word count (Article body): 5,129

Number of figures: 4

Number of tables: 1

Supplementary Material: Supplementary Methods, Supplementary Results, Supplementary Figures 1-6, Supplementary Tables 1-5

Abstract

Background: Transcranial direct current stimulation (tDCS) above the left dorsolateral prefrontal cortex (lDLPFC) has been widely used to improve symptoms of major depressive disorder (MDD). However, the effects of different stimulation protocols in the entire frontal lobe have not been investigated in a large sample including patient data.

Methods: We used 38 head models created from structural magnetic resonance imaging data of 19 healthy adults and 19 MDD patients and applied computational modeling to simulate the spatial distribution of tDCS-induced electric fields (EFs) in 20 frontal regions. We evaluated effects of seven bipolar and two multi-electrode 4x1 tDCS protocols.

Results: For bipolar montages, EFs were of comparable strength in the lDLPFC and in the medial prefrontal cortex (MPFC). Depending on stimulation parameters, EF cortical maps varied to a considerable degree, but were found to be similar in controls and patients. 4x1 montages produced more localized, albeit weaker effects.

Limitations: White matter anisotropy was not modeled. The relationship between EF strength and clinical response to tDCS could not be evaluated.

Conclusions: In addition to lDLPFC stimulation, excitability changes in the MPFC should also be considered as a potential mechanism underlying clinical efficacy of bipolar montages. MDD-associated anatomical variations are not likely to substantially influence current flow. Individual modeling of tDCS protocols can substantially improve cortical targeting. We make recommendations for future research to explicitly test the contribution of lDLPFC vs. MPFC stimulation to therapeutic outcomes of tDCS in this disorder.

Keywords: transcranial direct current stimulation; tDCS; depression; computational modeling; dorsolateral prefrontal cortex; medial prefrontal cortex

Background

Transcranial direct current stimulation (tDCS) is one of the most widespread non-invasive brain stimulation (NIBS) methods that have been used for alleviating symptoms of major depressive disorder (MDD). During conventional bipolar tDCS, two electrodes, an anode and a cathode, are placed on the head, and the stimulator is set to deliver weak (typically 1 or 2 mA) currents to the brain for 8-20 minutes (Filmer et al., 2014; Miniussi et al., 2013; Antal et al., 2017). Early animal studies provided evidence that polarizing currents applied to the cortical surface shift the resting membrane potential of pyramidal neurons in a polarity-dependent manner, which in turn can facilitate or inhibit their spontaneous and stimulus-evoked activity under the anode and cathode, respectively (Bindman et al., 1964; Purpura and McMurtry, 1965). In line with these findings, human studies have shown that tDCS induces polarity-specific effects in the motor or sensory cortex, although results are less consistent for prefrontal cortex (PFC) stimulation (Antal et al., 2003; Nitsche and Paulus, 2000; Tremblay et al., 2014).

TDCS is primarily applied above the left dorsolateral prefrontal cortex (lDLPFC) in MDD, a region that was shown to be hypoactive in this disorder (Fales et al., 2008; Grimm et al., 2008; Siegle et al., 2007). In healthy volunteers, anodal tDCS suppressed the evaluation of emotionally negative stimuli (Boggio et al., 2009; Maeoka et al., 2012; Peña-Gómez et al., 2011) and improved frustration tolerance in a demanding cognitive task (Plewnia et al., 2015a). Thus, it is reasonable to assume that by increasing excitability in the left DLPFC, dysfunctional control over negative thoughts and attentional bias towards negative stimuli can be restored in MDD patients, leading to significant improvement in symptomatology (Disner et al., 2011; Plewnia et al., 2015b; Rive et al., 2013). In support of this, successful pharmacotherapy, cognitive therapy or invasive brain stimulation have all been associated

with normalization (i.e., enhancement) of lDLPFC activity (Bench et al., 1995; DeRubeis et al., 2008; Mayberg et al., 2005).

Since the first report on the clinical efficacy of anodal tDCS over the lDLPFC in MDD (Fregni et al., 2006a), nine double-blind, sham-controlled studies were conducted involving more than 300 patients (Bennabi et al., 2015; Blumberger et al., 2012; Boggio et al., 2008; Brunoni et al., 2013, 2017, Loo et al., 2010, 2012, 2018; Palm et al., 2012). Still, only five studies reported significant improvements in symptoms severity when compared to sham stimulation (Boggio et al., 2008; Brunoni et al., 2013, 2017; Fregni et al., 2006a; Loo et al., 2012), which might be related to different sample sizes, dissimilarities between stimulation protocols, between-patient variations in brain anatomy and/or patient selection criteria. However, a recent meta-analysis that included individual patient data of six randomized, sham-controlled, double-blind trials provided clear evidence for the superiority of active tDCS versus sham stimulation (Brunoni et al., 2016a).

Studies reviewed so far offer a relatively straightforward model for understanding the clinical effects of tDCS in MDD: (1) in the healthy, the lDLPFC is involved in suppressing the influence of negative emotional stimuli on behavior, (2) the lDLPFC is hypoactive in depression, (3) processes linked to lDLPFC are implicated in the psychopathology of MDD, and (4) successful MDD treatment normalizes lDLPFC activity in MDD. Due to the fact that several studies have successfully used tDCS to influence neurophysiological and/or behavioral outcomes by placing the electrodes above the region of interest (Antal et al., 2003; Meinzer et al., 2012; Nitsche et al., 2007; Nitsche and Paulus, 2000), it is usually assumed that the primary effects of tDCS are manifested under the electrode pads. However, the spatial resolution of tDCS is rather poor: Given that the current flows from the anode towards the cathode, substantial effects should also be expected in brain areas situated between the two electrodes. This assertion was confirmed by modeling and neuroimaging studies, with

stimulation-induced electric fields (EFs) and hemodynamic responses being very strong in regions between the electrodes (Antal et al., 2011; Bai et al., 2014; Baudewig et al., 2001; Bikson et al., 2010a; Datta et al., 2009; Datta, 2012; Laakso et al., 2016; Lang et al., 2005; Miranda et al., 2013; Seibt et al., 2015). These results raise the possibility that tDCS-associated behavioral effects might also be linked to the stimulation of regions that are not intentionally targeted.

In this study, we used computational modeling to analyze the spatial distribution of EFs in realistic head models created from structural magnetic resonance imaging (MRI) scans of 19 healthy adults and 19 MDD patients. Simulations were performed on a relatively large cohort of participants because inter-individual differences in head and brain anatomy were shown to significantly influence current flow (Datta, 2012; Laakso et al., 2016; Opitz et al., 2015; Seibt et al., 2015). Given the evidence for systematic anatomical alterations in MDD (Bora et al., 2012; Kempton et al., 2011; Price and Drevets, 2010; Schmaal et al., 2017), we also included head models created from patient data to assess whether and to what extent healthy individuals and MDD patients differ in terms of the spatial distribution of tDCS-induced EFs in the brain. We compared the effects of five montages used in the six studies included in a recent meta-analysis because, when merged together in the individual patient data approach, these were shown to be significantly superior to sham stimulation in MDD (Brunoni et al., 2016a). In addition, we simulated the protocols of the two most recent double-blind randomized studies involving the largest patient groups so far (Brunoni et al., 2017; Loo et al., 2018). Based on earlier studies that implicated stronger EFs in regions between electrode pads, we expected to find robust stimulation-related effects outside the DLPFC (Bikson et al., 2010a; Datta et al., 2009; Miranda et al., 2013; Seibt et al., 2015). Finally, we simulated the effects of two 4x1 tDCS montages to make recommendations for an improved protocol with more selective targeting of MDD-associated areas (Datta et al., 2008, 2009).

Methods and Materials

Participants

High-resolution head models were created from T1-weighted anatomical images that were collected in a separate functional MRI study (Lepping et al., 2016). The data was obtained from the OpenfMRI database (https://openfmri.org/; accession number: ds000171). Structural scans of 19 healthy adult participants with no history of depression or other psychiatric disorders (11 females; mean±SD age: 28.79±10.86) and 19 unmedicated patients formerly diagnosed with MDD and experiencing a depressive episode at the time of the scanning (11 females; mean±SD age: 33.52±13.35) were used.[1] For full details regarding demographic data, we refer to the original paper (Lepping et al., 2016).

Creation of head models

The workflow for data extraction is shown in Figure 1. Except for four manual steps (see Supplementary Methods), all procedures were done in a fully automated manner, using a pipeline developed in Nipype (http://nipype.readthedocs.io/en/latest/) (Gorgolewski et al., 2011). Automated tissue segmentation was performed in SPM12 (Friston et al., 1994) for skin, skull, eyeballs and CSF, and in FreeSurfer (Fischl et al., 1999) for gray and white matter. We used an extended version of SimNIBS 2.0 (Thielscher et al., 2015), a freely available software package for simulating the effects of NIBS techniques (www.simnibs.org/) for creating the final head models. Head meshes consisted of approximately 3,200,000 tetrahedral elements, assigned to six tissue types (Supplementary Figure 1).

TDCS simulations and data extraction

[1] Data of one control participant ("sub-control20") was excluded due to technical problems with head model creation.

TDCS electrodes for the seven bipolar montages were sized and positioned as described in the original papers (Table 1). Electrode parameters and orientations are presented in Supplementary Methods). Head models for all participants and the consistency of electrode placement for one montage are shown in Supplementary Figure 2. For 4x1 montages, four surrounding cathodes were positioned around the central anode to form a circle with a radius of approximately 7 cm (Villamar et al., 2013). The central electrode was placed above the target region, which was either the lDLPFC (electrode F3) or the medial prefrontal cortex (MPFC; electrode Fz). The MPFC was chosen because our analysis for the bipolar montages indicated especially strong tDCS fields in this region.

After setting the current intensities for all montages[2] (Table 1), we ran field calculations based on the Finite Element Method (FEM) (Saturnino et al., 2015). Tissue conductivities are shown in Supplementary Table 1. The resulting spatial maps of tDCS-induced EF distributions for each participant and montage were saved as two-dimensional maps corresponding to the middle of the cortical sheets of individual head models, registered to the average surface ('fsaverage') of FreeSurfer. These reconstructed cortical surfaces were used for atlas-based automated parcellation of the frontal lobe into 20 regions (10 labels per hemisphere: primary motor cortex, lateral premotor cortex, supplementary motor cortex (SMC), frontal eye field (FEF), medial and lateral orbitofrontal cortex (MOFC, LOFC), inferior PFC, DLPFC, MPFC and anterior cingulate cortex (ACC)) (Ranta et al., 2009, 2014).

In order to compare the spatial distribution of EFs in different montages, EF cortical maps were normalized to individual maxima measured in the whole cortex. For analyzing inter-individual variability in the spatial distribution of EF "hotspots" (small regions with peak EFs), we created flattened cortical surfaces using Pycortex

[2] In the montage used by Palm et al. (2012), the stronger stimulation intensity of 2 mA was applied because this was associated with slightly better clinical outcome.

(https://github.com/gallantlab/pycortex) (Gao et al., 2015) to visualize the degree of hotspot overlap across individuals in the control and MDD groups separately. Hotspots were defined as nodes with peak 1% and 5% EF magnitude in the whole cortex. Montage-, label- and hemisphere-specific EF magnitude data were extracted for each participant for group analysis.

We quantified electric field strength in two ways: the absolute strength (vector norm) of the EF ($EF_{intensity}$) at each node is informative of the EF strength at that location, while the intensity of the EF component normal to the cortical surface (EF_{normal}) reflects currents either entering or leaving the cortex (i.e., with an orientation perpendicular to the cortical surface), being associated with polarity-specific (anodal- or cathodal-like) effects (Rahman et al., 2013). For both measures, label- and hemisphere-specific mean and peak values were obtained. Finally, we calculated a focality-index by quantifying the proportion on positive (inward-flowing) or negative (outward-flowing) peak 1% hotspots ($EF_{normal+}$ and $EF_{normal-}$, respectively) in certain regions (lDLPFC or bilateral MPFC) relative to the whole cortex. This index allowed montage comparison in terms of spatial selectivity (results reported in Supplementary Results).

Data analysis

We used Bayesian estimation methods for all reported analyses. These methods have many advantages over traditional null-hypothesis testing framework especially in an exploratory context with many variables such as ours, where the focus must necessarily lie on effect estimation rather than hypothesis testing (Gelman et al., 2014; Kruschke, 2010). In addition, Bayesian methods allow the quantification of both estimation and irreducible uncertainty at all levels (i.e., region, subject and group-levels), which is important to explore structure in the data. Also, computation of the full Bayesian posterior allows employing the most sophisticated model-selection criteria available to date (Vehtari et al., 2015). Full details of data analysis are described in Supplementary Methods. We report our results in terms of

posterior means and 95% highest-density intervals (HDIs), which reflect the range in which the estimated parameter is located with 95% probability.

Changes in EF strengths were analyzed by submitting mean $EF_{intensity}$ or EF_{normal} values to Bayesian hierarchical regression analysis (for details see Supplementary Methods). For the bipolar montages, we estimated all models that included all possible combinations of group (N=2), montage (N=7), label (N=10) and hemisphere (N=2) as well as all possible interactions between those variables as predictors (all dummy-coded), and let the intercept vary by subject. The intercepts were constrained by a group-level normal distribution with mean μ_a and standard deviation σ_a.

Non-informative (uniform) priors were placed on all variables. We used a model-selection strategy using the leave-one-out cross-validation information criterion (LOOIC), which resolves several of the difficulties of the deviance information criterion (Gelman et al., 2014; Vehtari et al., 2015; Watanabe, 2013). Differences in LOOIC larger than 10 can be considered strong (Pratte and Rouder, 2012). We followed the same strategy for the 4x1 tDCS montages, where we estimated all models that included a combination of group (N=2), montage (N=2, MPFC vs. lDLPFC), label (N=10) and hemisphere (N=2).

The EF strength was modeled as a function of montage, label, hemisphere and group (for bipolar and 4x1 montages separately), because we anticipated stimulation effects to vary across these dimensions, with the intercept accounting for between-subject variation regardless of group membership.

Results

Bipolar montages

Model selection for the hierarchical Bayesian regression analysis revealed that the model incorporating hemisphere, label and montage as predictors accounted best for the mean $EF_{intensity}$ and EF_{normal} distributions (Supplementary Tables 2-3).

The effect of label and hemisphere is not surprising, as cortical maps corresponding to $EF_{intensity}$ distributions indicated that tDCS-induced EFs were not restricted to the target lDLPFC region (see Figure 2 for three representative bipolar montages and Supplementary Figure 3 for the other four protocols). As expected, the overall effect of tDCS was also robust in non-targeted areas, primarily in bilateral MPFC, but also in the right DLPFC (rDLPFC) and the right LOFC (Supplementary Figure 4). For the EF_{normal}, a marked hemispheric effect was present: inward-flowing ($EF_{normal+}$) current magnitudes were comparable in the lateral surface of the left hemisphere and medial surface of the right hemisphere, and conversely, outward-flowing ($EF_{normal-}$) currents were of similar intensity in the medial surface of the left hemisphere and lateral surface of the right hemisphere. In line with this, mean EF_{normal} values were positive for the lDLPFC and left FEF, but also for the right MPFC, ACC, MOFC and SMC, indicating that on average, these regions received anodal-like stimulation, while cathodal-like effects ($EF_{normal} <0$) were dominant in the rDLPFC/right FEF, and the left MPFC, ACC, MOFC and SMC. This specific spatial distribution of normal currents can be expected when considering the direction of current flow in these montages: positive currents enter the lateral aspect of the left hemisphere near the anode, leave the cortex at the medial

surface of the same hemisphere, re-enter the cortex at the right medial surface, and leave the brain near the cathode, at the lateral aspect of the right hemisphere.[3]

With respect to the effect of montage, substantial differences were found between the seven bipolar montages. These were mainly due to the distinct effects of the Loo et al. (2010), Loo et al. (2012) and Loo (2018) protocols: given the weaker stimulation intensity (1 mA), EF strength was much lower in all regions for the Loo et al. (2010) montage, and the strongest stimulation intensity of 2.5 mA yielded opposite effects for the Loo et al. (2018) protocol. With respect to the montage by Loo et al. (2012, 2018), stronger excitatory ($EF_{normal+}$) effects were induced in the lateral and medial aspects of the right hemisphere in many cortical labels, including the ACC, MOFC and MPFC (Supplementary Figure 4). As for the lDLPFC, excitatory effects were equally strong in four montages (results regarding the focality-index are reported in Supplementary Results and shown in Supplementary Figure 5) (Bennabi et al., 2015; Blumberger et al., 2012; Brunoni et al., 2017, 2013; Palm et al., 2012).

Finally, an important finding was that group as predictor was never included into the winning model (Supplementary Tables 2-3), with the second-best model incorporating group as predictor differing from the winning model by at least >60 LOOIC units, suggesting that anatomical variations due to MDD diagnosis did not substantially contribute to the observed effects across regions. It is, however, possible that anatomical differences are manifest within cortical regions which cannot be picked up by our global analysis. In our more detailed analysis of the spatial distribution of EF_{normal} currents in labels receiving the strongest stimulation (i.e., the DLPFC and the MPFC) we found subtle group differences in the location of nodes with particularly high activities, being most prominent along the superior frontal

[3] We also note that cortical "stripes" with opposite sign of the EF_{normal} resembled the folding pattern of the cortex, which again was indicative of the direction of current flow being restricted by cortical anatomy (by the spatial distribution of gyri and sulci).

sulcus (Figure 3). Analysis of hotspot distributions yielded very similar results with respect to group differences for peak 1% and 5% hotspots (Figures 3 and Supplementary Figure 6).

4x1 montages

As anticipated, the 4x1 DLPFC protocol proved well-suited for a highly selective excitatory stimulation of the left hemisphere, peaking in the lDLPFC, and conversely, excitatory effects of the 4x1 MPFC montage were rather restricted to the MPFC (Figures 4 and Supplementary Figure 5). However, EF magnitudes were also smaller by around 25% for these montages (Figure 4). It is worth noting that the 4x1 DLPFC protocol also produced relatively strong $EF_{normal+}$ and $EF_{normal-}$ currents in the superior-lateral and medial surface of the left MPFC, respectively. Moreover, the 4x1 MPFC montage yielded high $EF_{normal+}$ values in the bilateral DLPFC and ACC.

For these two protocols, model selection indicated that label, hemisphere and montage were the best predictors of $EF_{intensity}$ and EF_{normal} parameters, but again, group was not included in the winning model (Supplementary Tables 4-5). Second-best models incorporating group as predictor were inferior to winning models by at least 30 LOOIC units, indicating substantially weaker model fit.

Discussion

We used realistic head models built from structural MRI scans to analyze the spatial selectivity of tDCS protocols that are most promising for alleviating the symptoms of MDD (Brunoni et al., 2016a). EF strength was quantified in 20 regions of the frontal lobe to look for latent effects in areas distant from the electrodes. Importantly, by including a relatively large number of head models derived from patient data, our study also enabled assessing how MDD-related neuropathology influenced current flow in the brain.

Stimulation of lDLPFC might not be related to clinical efficacy

Our results conform with previous computational modeling studies in that bipolar protocols are suitable for the stimulation of the lDLPFC (Bai et al., 2014; Ho et al., 2014; Laakso et al., 2016; Seibt et al., 2015). In addition to the lDLPFC, our simulations showed that traditional bipolar montages have also induced strong EF_{normal} currents in the bilateral FEF. FEF stimulation might also be related to improved cognitive control, since this region is part of the dorsal frontoparietal network, implicated in top-down control of attentional selection of environmental stimuli (Corbetta et al., 2008). Nevertheless, we argue that stimulation of lDLPFC/FEF might not be causally associated with symptom improvement in MDD. Firstly, although recent meta-analyses showed that anodal tDCS above the lDLPFC improves performance on tests of executive functioning and working memory in healthy adults and MDD patients (Brunoni et al., 2016b; Hill et al., 2016; Mancuso et al., 2016), the degree of cognitive improvement in MDD seems to be independent of the magnitude of clinical response, pointing towards independent mechanisms (Boggio et al., 2007; Brunoni et al., 2016b; Fregni et al., 2006b). The association between lDLPFC stimulation, cognitive enhancement and symptom alleviation is stronger for a more focal NIBS technique, repetitive transcranial magnetic stimulation (rTMS), since initial improvement in visuospatial working memory performance was pointed out as a significant predictor of subsequent clinical

response (Hoy et al., 2012). Secondly, strongest EFs in the lDLPFC were detected in the montage by Loo et al. (2018) (Supplementary Figure 4), despite the fact that to date this is the largest study with a negative outcome (i.e., comparable clinical effects for real vs. sham tDCS). Also, the focality-index for the lDLPFC in the montage by Brunoni et al. (2017) was relatively low, indicating that selective stimulation of this region is not absolutely necessary for symptom improvement. Finally, there is converging literature highlighting the MPFC, a region characterized by strong tDCS-induced EFs in our study, as one of the most promising novel targets for non-invasive stimulation in MDD (Downar and Daskalakis, 2013).

MPFC stimulation as a possible mechanism for clinical efficacy

Our most important finding concerns the strong stimulation of regions in the medial surface of the PFC (bilateral MPFC, ACC, MOFC) in every bipolar montage. At first glance, this result is not very surprising given the well-established poor spatial resolution of tDCS (Bikson et al., 2010b; Datta et al., 2009; Miranda et al., 2013; Saturnino et al., 2015), and similar effects were also noted by previous modeling and neuroimaging studies (Bai et al., 2014; Ho et al., 2014; Keeser et al., 2011; Laakso et al., 2016; Peña-Gómez et al., 2012; Seibt et al., 2015). Still, while neuroimaging studies have attributed distant effects to the stimulation of the lDLPFC and to the consequential perturbation of the intrinsic organization of complex brain networks (Deco et al., 2011), we show that even direct stimulation of the MPFC, ACC and MOFC is around the same magnitude as that of the lDLPFC. This raises the possibility that excitability changes in these regions contributed to the observed clinical effects of "DLPFC-targeting" bipolar tDCS protocols.

The MPFC has been implicated in downregulation of emotional reactions especially when participants used reappraisal strategies, a key element of cognitive therapy (Buhle et al., 2014; Disner et al., 2011; Etkin et al., 2015; Goldin et al., 2008; Kim and Hamann, 2007; Ochsner et al., 2004). Abnormal hemodynamic responses in MPFC have been consistently

shown in MDD patients, associated with failures in both automatic and voluntary emotion regulation (Kaiser et al., 2015; Rive et al., 2013; Taylor et al., 2008). Crucially, the dorsal part of the MPFC (DMPFC, the area receiving strongest stimulation in our bipolar montages) has been highlighted as a unique region characterized by increased connectivity with three large-scaled networks (cognitive control network, default mode network, affective network) in MDD, and linked to symptoms such as impaired executive functioning, rumination, increased self-focus and emotional dysregulation (Sheline et al., 2010).

From another perspective, MDD is characterized by altered sensitivity to reward and punishment, which might underlie impaired value-based decision-making in patients, typically observed in reinforcement learning (RL) paradigms (Chase et al., 2010; Chen et al., 2015; Eshel and Roiser, 2010; Huys et al., 2013; Pizzagalli et al., 2005). The MPFC/ACC/MOFC play key roles in RL (Cavanagh and Frank, 2014; Silvetti et al., 2014), and interestingly, the DMPFC shows enhanced activity during probabilistic reversal learning after serotonin (5-HT) depletion in healthy volunteers, a phenomenon associated with elevated punishment sensitivity in these individuals (Evers et al., 2005). This is particularly relevant to the context of impaired RL in MDD, because serotoninergic dysfunction in patients has also been linked to maladaptive choices in the face of future losses (Dayan and Huys, 2008; Huys et al., 2016).

Taken together, medial PFC regions have been linked to MDD though several psychological phenomena (emotion regulation, value-based decision-making and RL) and neural substrates (brain networks, serotoninergic neurotransmission). It is therefore no wonder that by targeting the DMPFC with rTMS, recent studies achieved significant symptom reduction in MDD (Downar et al., 2014; Salomons et al., 2014; Schulze et al., 2016). Based on our simulations, we therefore argue that conventional bipolar tDCS protocols have

inadvertently stimulated medial PFC structures as well and modulated cognitive processes associated with this area.

Our simulations also indicated a strong hemispheric lateralization for the bipolar electrode arrangements both in lateral and medial regions. Regarding the DLPFC/FEF, the dominance of inward (positive) and outward (negative) currents in the left and right hemisphere respectively, fits well to the DLPFC left-lateralized hypoactivity/right-lateralized hyperactivity model of MDD (Grimm et al., 2008). In the case of MPFC/ACC/MOFC, however, the preponderance of negative (putatively inhibitory) currents in the left relative to positive (putatively excitatory) currents in the right hemisphere is more difficult to interpret. As noted earlier, connectivity patterns of the DMPFC implicated this region in disrupted coordination between three resting-state functional networks in MDD, albeit without any hemispheric lateralization (Sheline et al., 2010). In theory, increased functional coupling between the DMPFC and functional networks could be normalized by reducing neural excitability in this region, an effect that we observed in the left hemisphere only. Perhaps, left-lateralized inhibitory ($EF_{normal-}$) currents are more relevant for symptom improvement, as only the left (but not right) DMPFC was reported to show reduced resting-state metabolism in MDD patients responding to either pharmacotherapy or cognitive behavior therapy (Kennedy et al., 2007). The fact that activity in the subgenual ACC is increased in MDD, but normalized after successful invasive stimulation (Lozano et al., 2008; Mayberg et al., 2005) also highlights the left-lateralized inhibitory effect as a strong candidate for the clinically relevant outcome.

Bipolar montages induce different EF patterns in the frontal lobe

Montage was a strong predictor of the calculated EF distributions in the winning statistical models, implying that stimulation parameters influence current flow substantially even though the position of the anode is fixed. With respect to normalized cortical maps

(Figures 2 and Supplementary Figure 3), the protocols by Loo et al. (2012, 2018) produced highly different EF patterns in both hemispheres, with less focal effects in DLPFC or MPFC (Supplementary Figure 5). We believe that the more widespread and right-lateralized effect was caused by the inferior-lateral scalp position of the cathode (placed at position F8), allowing currents to flow through a large cortical area in this hemisphere. Interestingly, out of the seven tDCS protocols, only three were associated with significant real vs. sham clinical effects (Brunoni et al., 2013, 2017; Loo et al., 2012), meaning that protocols with almost indistinguishable EF patterns (e.g., Brunoni et al. (2013) vs. Blumberger et al. (2012)) do not necessarily yield similar clinical outcomes, and conversely, protocols that seem to differ in their neural mechanisms can still lead to symptom improvement, i.e., Brunoni et al. (2013, 2017) vs. Loo et al. (2012). This can be explained by the large variety of brain abnormalities associated with this disorder (Kempton et al., 2011; Price and Drevets, 2010; Schmaal et al., 2017), but perhaps even more importantly, with the different patient selection criteria in these studies. For example, while Blumberger and colleagues (2012) recruited patients with severe depression, including those resistant to electroconvulsive therapy, the studies by Brunoni et al. (2013, 2017) included patients with relatively low degree of refractoriness. Therefore, in addition to careful stimulation parameter selection, other factors such as concomitant pharmacotherapy, symptom severity or treatment resistance can all contribute to the clinical efficacy of tDCS in MDD (Brunoni et al., 2016b).

TDCS effects are very similar in healthy individuals and MDD patients

With respect to between-group differences, we found largely similar EF maps for healthy individuals and MDD patients. This indicates that the cortical flow of currents is not substantially influenced by anatomical alterations associated with this disorder. Nevertheless, it is possible that more nuanced, systematic differences in the distribution of the EFs exist within the segmented cortical regions as our statistical model resolves only differences

between regions. When looking at the spatial distribution of hotspots within the four regions of interest (bilateral DLPFC and MPFC), we identified subtle differences between the two groups, since some cortical nodes were more likely to receive strong stimulation in the control group, whereas others were more affected by tDCS in patients. At this point, it is not clear if this phenomenon would be related to any behavioral tDCS-related effect, because such detailed delineation of the functional properties of subregions within the human DLPFC or MPFC is not available. Yet, this observation implies that spatial characteristics of tDCS within target areas should be considered when assessing differences in stimulation effects between different groups of participants.

Implications for future studies

So far, we argued that studies using conventional bipolar tDCS protocols aimed at targeting the lDLPFC should take the potential effects of MPFC stimulation into account. However, due to strong EFs in the lDLPFC, it seems to be rather difficult to disentangle the degree to which DLPFC and MPFC stimulation contributes to clinical efficacy. We acknowledge that the arguments favoring the MPFC in terms of antidepressive effects are speculative at this point, but they also offer testable predictions for future research. We therefore propose comparing the effects of lDLPFC- and MPFC-targeting 4x1 protocols by assessing changes in behavioral performance with cognitive tasks associated with the activity of these regions (i.e., cognitive control tasks for DLPFC vs. RL paradigms for MPFC) (Chase et al., 2010; Pizzagalli et al., 2005; Salehinejad et al., 2017; Wolkenstein and Plewnia, 2013).

Limitations

The main limitation of our study is that it is purely based on computational simulations of head anatomy and current flow, and therefore, provides only a rough approximation of the neural effects that can be expected in a real clinical setting. Perhaps most importantly, our

head models consisted of tissues with isotropic conductivities, which might be especially problematic for the white matter. Still, a recent study found that modeling white matter anisotropy primarily influenced current density in deeper structures, while leaving superficial gray matter targets relatively unaffected (Wagner et al., 2014).

Our models of EF distribution in the cortex are static as they do not account for the temporal dynamics of stimulation effects. TDCS-associated currents were shown to influence the cerebral vasculature in a polarity-dependent manner (Giorli et al., 2015), that can also impact neural excitability and change tissue impedance during tDCS sessions. However, to the best of our knowledge, such effects have not yet been incorporated into any computational model of brain stimulation thus far.

Another limitation is that our dataset did not enable assessing the relationship between EF strength in target regions (i.e., in the lDLPFC and in bilateral MPFC) and the magnitude of clinical response to tDCS in patients. Since standard deviations for both mean and peak EF values were rather large in these cortical labels (Figures 2, 4 and Supplementary Figure 3), we can assume that between-patient variability in the degree of tDCS-related symptom improvement is at least partially related to stimulation strength in target regions (in addition to other factors such as refractoriness to previous therapeutic interventions). We think that this issue can be directly assessed in the future by simultaneously performing patient stimulation and EF modeling in the same cohort of participants.

Conclusions

TDCS is a promising tool for alleviating symptoms of several neurological and psychiatric brain disorders (Antal et al., 2017; Filmer et al., 2014; Hill et al., 2016). However, its mechanism of action is not well understood, and the considerably large number of negative studies might be related to non-optimal stimulation protocols (Tremblay et al., 2014). Our

results underline the utility of computational modeling for elucidating the neural underpinnings of tDCS and uncovering potentially hidden effects (Datta et al., 2009; Miniussi et al., 2013; Miranda et al., 2013; Opitz et al., 2015). By using structural scans of patients, it is now possible to simulate the effects of NIBS on individual head models. This approach might enable the development of personalized interventional protocols, leading to more precise cortical targeting and an increased potential for achieving clinical efficacy.

Data Availability Statement

All analysis scripts, individual and group-averaged anatomical cortical surfaces with PFC labels and montage-specific $EF_{intensity}$ and EF_{normal} cortical maps are available for download at https://osf.io/u5brq/.

Author Contributions

Gábor Csifcsák, Nya Mehnwolo Boayue and Matthias Mittner conceived the study design.

Gábor Csifcsák, Nya Mehnwolo Boayue and Oula Puonti contributed to head model creation.

Nya Mehnwolo Boayue performed the simulations.

Nya Mehnwolo Boayue and Matthias Mittner contributed to data extraction.

Axel Thielscher oversaw the data extraction procedure.

Matthias Mittner performed the statistical analysis.

All authors contributed to manuscript preparation.

Role of Funding Source and Acknowledgements

This work was supported by the Northern Norway Regional Health Authority (grant no. PFP1237-15) for GC and MM and by the Lundbeck foundation (grant no. R118-A11308) and the Novonordisk foundation (grant no. NNF14OC0011413) for OP and AT. We thank Steward Mostofsky, Deana Crocetti, Benjamin Dirlikov and Jina Pakpoor for providing the atlas for parcellation of the frontal lobe.

Declaration of Interest

Declarations of interest: none.

References

Antal, A., Alekseichuk, I., Bikson, M., Brockmöller, J., Brunoni, A.R., Chen, R., Cohen, L.G., Dowthwaite, G., Ellrich, J., Flöel, A., 2017. Low intensity transcranial electric stimulation: Safety, ethical, legal regulatory and application guidelines. Clin. Neurophysiol. 128, 1774–1809.

Antal, A., Kincses, T.Z., Nitsche, M.A., Paulus, W., 2003. Manipulation of phosphene thresholds by transcranial direct current stimulation in man. Exp. Brain Res. 150, 375–378.

Antal, A., Polania, R., Schmidt-Samoa, C., Dechent, P., Paulus, W., 2011. Transcranial direct current stimulation over the primary motor cortex during fMRI. NeuroImage 55, 590–596.

Bai, S., Dokos, S., Ho, K.-A., Loo, C., 2014. A computational modelling study of transcranial direct current stimulation montages used in depression. Neuroimage 87, 332–344.

Baudewig, J., Nitsche, M.A., Paulus, W., Frahm, J., 2001. Regional modulation of BOLD MRI responses to human sensorimotor activation by transcranial direct current stimulation. Magn. Reson. Med. 45, 196–201.

Bench, C.J., Frackowiak, R.S., Dolan, R.J., 1995. Changes in regional cerebral blood flow on recovery from depression. Psychol. Med. 25, 247–261.

Bennabi, D., Nicolier, M., Monnin, J., Tio, G., Pazart, L., Vandel, P., Haffen, E., 2015. Pilot study of feasibility of the effect of treatment with tDCS in patients suffering from treatment-resistant depression treated with escitalopram. Clin. Neurophysiol. 126, 1185–1189.

Bikson, M., Datta, A., Rahman, A., Scaturro, J., 2010a. Electrode montages for tDCS and weak transcranial electrical stimulation: Role of return electrode's position and size. Clin. Neurophysiol. 121, 1976–1978.

Bikson, M., Datta, A., Rahman, A., Scaturro, J., 2010b. Electrode montages for tDCS and weak transcranial electrical stimulation: role of "return" electrode's position and size. Clin. Neurophysiol. 121, 1976–1978.

Bindman, L.J., Lippold, O.C.J., Redfearn, J.W.T., 1964. The action of brief polarizing currents on the cerebral cortex of the rat (1) during current flow and (2) in the production of long-lasting after-effects. J. Physiol. 172, 369–382.

Blumberger, D.M., Tran, L.C., Fitzgerald, P.B., Hoy, K.E., Daskalakis, Z.J., 2012. A randomized double-blind sham-controlled study of transcranial direct current stimulation for treatment-resistant major depression. Front. Psychiatry 3, 74.

Boggio, P.S., Bermpohl, F., Vergara, A.O., Muniz, A.L., Nahas, F.H., Leme, P.B., Rigonatti, S.P., Fregni, F., 2007. Go-no-go task performance improvement after anodal transcranial DC stimulation of the left dorsolateral prefrontal cortex in major depression. J. Affect. Disord. 101, 91–98.

Boggio, P.S., Rigonatti, S.P., Ribeiro, R.B., Myczkowski, M.L., Nitsche, M.A., Pascual-Leone, A., Fregni, F., 2008. A randomized, double-blind clinical trial on the efficacy of cortical direct current stimulation for the treatment of major depression. Int. J. Neuropsychopharmacol. 11, 249–254.

Boggio, P.S., Zaghi, S., Fregni, F., 2009. Modulation of emotions associated with images of human pain using anodal transcranial direct current stimulation (tDCS). Neuropsychologia 47, 212–217.

Bora, E., Fornito, A., Pantelis, C., Yücel, M., 2012. Gray matter abnormalities in Major Depressive Disorder: A meta-analysis of voxel based morphometry studies. J. Affect. Disord. 138, 9–18.

Brunoni, A.R., Moffa, A.H., Fregni, F., Palm, U., Padberg, F., Blumberger, D.M., Daskalakis, Z.J., Bennabi, D., Haffen, E., Alonzo, A., others, 2016a. Transcranial direct current stimulation for acute major depressive episodes: meta-analysis of individual patient data. Br. J. Psychiatry 208, 522–531.

Brunoni, A.R., Moffa, A.H., Sampaio-Junior, B., Borrione, L., Moreno, M.L., Fernandes, R.A., Veronezi, B.P., Nogueira, B.S., Aparicio, L.V.M., Razza, L.B., 2017. Trial of Electrical Direct-Current Therapy versus Escitalopram for Depression. N. Engl. J. Med. 376, 2523–2533.

Brunoni, A.R., Tortella, G., Benseñor, I.M., Lotufo, P.A., Carvalho, A.F., Fregni, F., 2016b. Cognitive effects of transcranial direct current stimulation in depression: Results from the SELECT-TDCS trial and insights for further clinical trials. J. Affect. Disord. 202, 46–52.

Brunoni, A.R., Valiengo, L., Baccaro, A., Zanão, T.A., de Oliveira, J.F., Goulart, A., Boggio, P.S., Lotufo, P.A., Benseñor, I.M., Fregni, F., 2013. The sertraline vs. electrical current therapy for treating depression clinical study: results from a factorial, randomized, controlled trial. JAMA Psychiatry 70, 383–391.

Buhle, J.T., Silvers, J.A., Wager, T.D., Lopez, R., Onyemekwu, C., Kober, H., Weber, J., Ochsner, K.N., 2014. Cognitive reappraisal of emotion: a meta-analysis of human neuroimaging studies. Cereb. Cortex 24, 2981–2990.

Cavanagh, J.F., Frank, M.J., 2014. Frontal theta as a mechanism for cognitive control. Trends Cogn. Sci. 18, 414–421.

Chase, H.W., Frank, M.J., Michael, A., Bullmore, E.T., Sahakian, B.J., Robbins, T.W., 2010. Approach and avoidance learning in patients with major depression and healthy controls: relation to anhedonia. Psychol. Med. 40, 433–440.

Chen, C., Takahashi, T., Nakagawa, S., Inoue, T., Kusumi, I., 2015. Reinforcement learning in depression: a review of computational research. Neurosci. Biobehav. Rev. 55, 247–267.

Corbetta, M., Patel, G., Shulman, G.L., 2008. The reorienting system of the human brain: from environment to theory of mind. Neuron 58, 306–324. https://doi.org/10.1016/j.neuron.2008.04.017

Datta, A., 2012. Inter-Individual Variation during Transcranial Direct Current Stimulation and Normalization of Dose Using MRI-Derived Computational Models. Front. Psychiatry 3, 91.

Datta, A., Bansal, V., Diaz, J., Patel, J., Reato, D., Bikson, M., 2009. Gyri-precise head model of transcranial direct current stimulation: improved spatial focality using a ring electrode versus conventional rectangular pad. Brain Stimulat. 2, 201–207.

Datta, A., Elwassif, M., Battaglia, F., Bikson, M., 2008. Transcranial current stimulation focality using disc and ring electrode configurations: FEM analysis. J Neural Eng 5, 163–174.

Dayan, P., Huys, Q.J., 2008. Serotonin, inhibition, and negative mood. PLoS Comput. Biol. 4, e4.

Deco, G., Jirsa, V.K., McIntosh, A.R., 2011. Emerging concepts for the dynamical organization of resting-state activity in the brain. Nat. Rev. Neurosci. 12, 43–56.

DeRubeis, R.J., Siegle, G.J., Hollon, S.D., 2008. Cognitive therapy versus medication for depression: treatment outcomes and neural mechanisms. Nat. Rev. Neurosci. 9, 788–796.

Disner, S.G., Beevers, C.G., Haigh, E.A., Beck, A.T., 2011. Neural mechanisms of the cognitive model of depression. Nat. Rev. Neurosci. 12, 467–477.

Downar, J., Daskalakis, Z.J., 2013. New targets for rTMS in depression: a review of convergent evidence. Brain Stimulat. 6, 231–240.

Downar, J., Geraci, J., Salomons, T.V., Dunlop, K., Wheeler, S., McAndrews, M.P., Bakker, N., Blumberger, D.M., Daskalakis, Z.J., Kennedy, S.H., others, 2014. Anhedonia and reward-circuit connectivity distinguish nonresponders from responders to dorsomedial prefrontal repetitive transcranial magnetic stimulation in major depression. Biol. Psychiatry 76, 176–185.

Eshel, N., Roiser, J.P., 2010. Reward and punishment processing in depression. Biol. Psychiatry 68, 118–124.

Etkin, A., Büchel, C., Gross, J.J., 2015. The neural bases of emotion regulation. Nat. Rev. Neurosci. 16, 693–700.

Evers, E.A., Cools, R., Clark, L., van der Veen, F.M., Jolles, J., Sahakian, B.J., Robbins, T.W., 2005. Serotonergic Modulation of Prefrontal Cortex during Negative Feedback in Probabilistic Reversal Learning. Neuropsychopharmacology 30, 1138–1147.

Fales, C.L., Barch, D.M., Rundle, M.M., Mintun, M.A., Snyder, A.Z., Cohen, J.D., Mathews, J., Sheline, Y.I., 2008. Altered emotional interference processing in affective and cognitive-control brain circuitry in major depression. Biol. Psychiatry 63, 377–384.

Filmer, H.L., Dux, P.E., Mattingley, J.B., 2014. Applications of transcranial direct current stimulation for understanding brain function. Trends Neurosci. 37, 742–753.
Fischl, B., Sereno, M.I., Dale, A.M., 1999. Cortical surface-based analysis: II: inflation, flattening, and a surface-based coordinate system. Neuroimage 9, 195–207.
Fregni, F., Boggio, P.S., Nitsche, M.A., Marcolin, M.A., Rigonatti, S.P., Pascual-Leone, A., 2006a. Treatment of major depression with transcranial direct current stimulation. Bipolar Disord. 8, 203–204.
Fregni, F., Boggio, P.S., Nitsche, M.A., Rigonatti, S.P., Pascual-Leone, A., 2006b. Cognitive effects of repeated sessions of transcranial direct current stimulation in patients with depression. Depress. Anxiety 23, 482–484.
Friston, K.J., Holmes, A.P., Worsley, K.J., Poline, J.-P., Frith, C.D., Frackowiak, R.S., 1994. Statistical parametric maps in functional imaging: a general linear approach. Hum. Brain Mapp. 2, 189–210.
Gao, J.S., Huth, A.G., Lescroart, M.D., Gallant, J.L., 2015. Pycortex: an interactive surface visualizer for fMRI. Front. Neuroinformatics 9, 23.
Gelman, A., Hwang, J., Vehtari, A., 2014. Understanding predictive information criteria for Bayesian models. Stat. Comput. 24, 997–1016.
Giorli, E., Tognazzi, S., Briscese, L., Bocci, T., Mazzatenta, A., Priori, A., Orlandi, G., Del Sette, M., Sartucci, F., 2015. Transcranial direct current stimulation and cerebral vasomotor reserve: a study in healthy subjects. J. Neuroimaging 25, 571–574.
Goldin, P.R., McRae, K., Ramel, W., Gross, J.J., 2008. The neural bases of emotion regulation: reappraisal and suppression of negative emotion. Biol. Psychiatry 63, 577–586.
Gorgolewski, K., Burns, C.D., Madison, C., Clark, D., Halchenko, Y.O., Waskom, M.L., Ghosh, S.S., 2011. Nipype: A Flexible, Lightweight and Extensible Neuroimaging Data Processing Framework in Python. Front. Neuroinformatics 5, 13.
Grimm, S., Beck, J., Schuepbach, D., Hell, D., Boesiger, P., Bermpohl, F., Niehaus, L., Boeker, H., Northoff, G., 2008. Imbalance between left and right dorsolateral prefrontal cortex in major depression is linked to negative emotional judgment: an fMRI study in severe major depressive disorder. Biol. Psychiatry 63, 369–376.
Hill, A.T., Fitzgerald, P.B., Hoy, K.E., 2016. Effects of Anodal Transcranial Direct Current Stimulation on Working and Recognition Memory: A Systematic Review and Meta-Analysis of Findings from Healthy and Neuropsychiatric Populations. Brain Stimulat. 2, 197–208.
Ho, K.-A., Bai, S., Martin, D., Alonzo, A., Dokos, S., Puras, P., Loo, C.K., 2014. A pilot study of alternative transcranial direct current stimulation electrode montages for the treatment of major depression. J. Affect. Disord. 167, 251–258.
Hoy, K.E., Segrave, R.A., Daskalakis, Z.J., Fitzgerald, P.B., 2012. Investigating the relationship between cognitive change and antidepressant response following rTMS: a large scale retrospective study. Brain Stimulat. 5, 539–546.
Huys, Q.J., Gölzer, M., Friedel, E., Heinz, A., Cools, R., Dayan, P., Dolan, R.J., 2016. The specificity of Pavlovian regulation is associated with recovery from depression. Psychol. Med. 46, 1027–1035.
Huys, Q.J., Pizzagalli, D.A., Bogdan, R., Dayan, P., 2013. Mapping anhedonia onto reinforcement learning: a behavioural meta-analysis. Biol. Mood Anxiety Disord. 3, 12.
Kaiser, R.H., Andrews-Hanna, J.R., Wager, T.D., Pizzagalli, D.A., 2015. Large-Scale Network Dysfunction in Major Depressive Disorder: A Meta-analysis of Resting-State Functional Connectivity. JAMA Psychiatry 72, 603–611.
Keeser, D., Meindl, T., Bor, J., Palm, U., Pogarell, O., Mulert, C., Brunelin, J., Möller, H.-J., Reiser, M., Padberg, F., 2011. Prefrontal Transcranial Direct Current Stimulation Changes Connectivity of Resting-State Networks during fMRI. J. Neurosci. 31, 15284–15293.
Kempton, M.J., Salvador, Z., Munafò, M.R., Geddes, J.R., Simmons, A., Frangou, S., Williams, S.C., 2011. Structural neuroimaging studies in major depressive disorder. Meta-analysis and comparison with bipolar disorder. Arch. Gen. Psychiatry 68, 675–690.

Kennedy, S.H., Konarski, J.Z., Segal, Z.V., Lau, M.A., Bieling, P.J., McIntyre, R.S., Mayberg, H.S., 2007. Differences in brain glucose metabolism between responders to CBT and venlafaxine in a 16-week randomized controlled trial. Am. J. Psychiatry 164, 778.

Kim, S.H., Hamann, S., 2007. Neural correlates of positive and negative emotion regulation. J. Cogn. Neurosci. 19, 776–798.

Kruschke, J.K., 2010. What to believe: Bayesian methods for data analysis. Trends Cogn. Sci. 14, 293–300.

Laakso, I., Tanaka, S., Mikkonen, M., Koyama, S., Sadato, N., Hirata, A., 2016. Electric fields of motor and frontal tDCS in a standard brain space: a computer simulation study. Neuroimage 137, 140–151.

Lang, N., Siebner, H.R., Ward, N.S., Lee, L., Nitsche, M.A., Paulus, W., Rothwell, J.C., Lemon, R.N., Frackowiak, R.S., 2005. How does transcranial DC stimulation of the primary motor cortex alter regional neuronal activity in the human brain? Eur. J. Neurosci. 22, 495–504.

Lepping, R.J., Atchley, R.A., Chrysikou, E., Martin, L.E., Clair, A.A., Ingram, R.E., Simmons, W.K., Savage, C.R., 2016. Neural Processing of Emotional Musical and Nonmusical Stimuli in Depression. PloS One 11, e0156859.

Loo, C.K., Alonzo, A., Martin, D., Mitchell, P.B., Galvez, V., Sachdev, P., 2012. Transcranial direct current stimulation for depression: 3-week, randomised, sham-controlled trial. Br. J. Psychiatry 200, 52–59.

Loo, C.K., Husain, M.M., McDonald, W.M., Aaronson, S., O'Reardon, J.P., Alonzo, A., Weickert, C.S., Martin, D.M., McClintock, S.M., Mohan, A., 2018. International randomized-controlled trial of transcranial Direct Current Stimulation in depression. Brain Stimulat. 11, 125–133.

Loo, C.K., Sachdev, P., Martin, D., Pigot, M., Alonzo, A., Malhi, G.S., Lagopoulos, J., Mitchell, P., 2010. A double-blind, sham-controlled trial of transcranial direct current stimulation for the treatment of depression. Int. J. Neuropsychopharmacol. 13, 61–69.

Lozano, A.M., Mayberg, H.S., Giacobbe, P., Hamani, C., Craddock, R.C., Kennedy, S.H., 2008. Subcallosal cingulate gyrus deep brain stimulation for treatment-resistant depression. Biol. Psychiatry 64, 461–467.

Maeoka, H., Matsuo, A., Hiyamizu, M., Morioka, S., Ando, H., 2012. Influence of transcranial direct current stimulation of the dorsolateral prefrontal cortex on pain related emotions: a study using electroencephalographic power spectrum analysis. Neurosci. Lett. 512, 12–16.

Mancuso, L.E., Ilieva, I.P., Hamilton, R.H., Farah, M.J., 2016. Does Transcranial Direct Current Stimulation Improve Healthy Working Memory?: A Meta-analytic Review. J. Cogn. Neurosci. 28, 1063–1089.

Mayberg, H.S., Lozano, A.M., Voon, V., McNeely, H.E., Seminowicz, D., Hamani, C., Schwalb, J.M., Kennedy, S.H., 2005. Deep brain stimulation for treatment-resistant depression. Neuron 45, 651–660.

Meinzer, M., Antonenko, D., Lindenberg, R., Hetzer, S., Ulm, L., Avirame, K., Flaisch, T., Flöel, A., 2012. Electrical Brain Stimulation Improves Cognitive Performance by Modulating Functional Connectivity and Task-Specific Activation. J. Neurosci. 32, 1859–1866.

Miniussi, C., Harris, J.A., Ruzzoli, M., 2013. Modelling non-invasive brain stimulation in cognitive neuroscience. Neurosci. Biobehav. Rev. 37, 1702–1712.

Miranda, P.C., Mekonnen, A., Salvador, R., Ruffini, G., 2013. The electric field in the cortex during transcranial current stimulation. Neuroimage 70, 48–58.

Nitsche, M.A., Doemkes, S., Karaköse, T., Antal, A., Liebetanz, D., Lang, N., Tergau, F., Paulus, W., 2007. Shaping the effects of transcranial direct current stimulation of the human motor cortex. J. Neurophysiol. 97, 3109–3117.

Nitsche, M.A., Paulus, W., 2000. Excitability changes induced in the human motor cortex by weak transcranial direct current stimulation. J. Physiol. 527, 633–639.

Ochsner, K.N., Ray, R.D., Cooper, J.C., Robertson, E.R., Chopra, S., Gabrieli, J.D., Gross, J.J., 2004. For better or for worse: neural systems supporting the cognitive down-and up-regulation of negative emotion. NeuroImage 23, 483–499.

Opitz, A., Paulus, W., Will, S., Antunes, A., Thielscher, A., 2015. Determinants of the electric field during transcranial direct current stimulation. Neuroimage 109, 140–150.
Palm, U., Schiller, C., Fintescu, Z., Obermeier, M., Keeser, D., Reisinger, E., Pogarell, O., Nitsche, M.A., Möller, H.J., Padberg, F., 2012. Transcranial direct current stimulation in treatment resistant depression: a randomized double-blind, placebo-controlled study. Brain Stimulat. 5, 242–251.
Peña-Gómez, C., Sala-Lonch, R., Junqué, C., Clemente, I.C., Vidal, D., Bargalló, N., Falcón, C., Valls-Solé, J., Pascual-Leone, Á., Bartrés-Faz, D., 2012. Modulation of large-scale brain networks by transcranial direct current stimulation evidenced by resting-state functional MRI. Brain Stimulat. 5, 252–263.
Peña-Gómez, C., Vidal-Piñeiro, D., Clemente, I.C., Pascual-Leone, Á., Bartrés-Faz, D., 2011. Down-regulation of negative emotional processing by transcranial direct current stimulation: effects of personality characteristics. PloS One 6, e22812.
Pizzagalli, D.A., Jahn, A.L., O'Shea, J.P., 2005. Toward an objective characterization of an anhedonic phenotype: a signal-detection approach. Biol. Psychiatry 57, 319–327.
Plewnia, C., Schroeder, P.A., Kunze, R., Faehling, F., Wolkenstein, L., 2015a. Keep calm and carry on: improved frustration tolerance and processing speed by transcranial direct current stimulation (tDCS). PloS One 10, e0122578.
Plewnia, C., Schroeder, P.A., Wolkenstein, L., 2015b. Targeting the biased brain: non-invasive brain stimulation to ameliorate cognitive control. Lancet Psychiatry 2, 351–356.
Pratte, M.S., Rouder, J.N., 2012. Assessing the dissociability of recollection and familiarity in recognition memory. J. Exp. Psychol. Learn. Mem. Cogn. 38, 1591–1607.
Price, J.L., Drevets, W.C., 2010. Neurocircuitry of Mood Disorders. Neuropsychopharmacology 35, 192–216.
Purpura, D.P., McMurtry, J.G., 1965. Intracellular activities and evoked potential changes during polarization of motor cortex. J. Neurophysiol. 28, 166–185.
Rahman, A., Reato, D., Arlotti, M., Gasca, F., Datta, A., Parra, L.C., Bikson, M., 2013. Cellular effects of acute direct current stimulation: somatic and synaptic terminal effects. J. Physiol. 591, 2563–2578.
Ranta, M.E., Chen, M., Crocetti, D., Prince, J.L., Subramaniam, K., Fischl, B., Kaufmann, W.E., Mostofsky, S.H., 2014. Automated MRI parcellation of the frontal lobe. Hum. Brain Mapp. 35, 2009–2026.
Ranta, M.E., Crocetti, D., Clauss, J.A., Kraut, M.A., Mostofsky, S.H., Kaufmann, W.E., 2009. Manual MRI parcellation of the frontal lobe. Psychiatry Res. 172, 147–154.
Rive, M.M., van Rooijen, G., Veltman, D.J., Phillips, M.L., Schene, A.H., Ruhé, H.G., 2013. Neural correlates of dysfunctional emotion regulation in major depressive disorder. A systematic review of neuroimaging studies. Neurosci. Biobehav. Rev. 37, 2529–2553.
Salehinejad, M.A., Ghanavai, E., Rostami, R., Nejati, V., 2017. Cognitive control dysfunction in emotion dysregulation and psychopathology of major depression (MD): Evidence from transcranial brain stimulation of the dorsolateral prefrontal cortex (DLPFC). J. Affect. Disord. 210, 241–248.
Salomons, T.V., Dunlop, K., Kennedy, S.H., Flint, A., Geraci, J., Giacobbe, P., Downar, J., 2014. Resting-state cortico-thalamic-striatal connectivity predicts response to dorsomedial prefrontal rTMS in major depressive disorder. Neuropsychopharmacology 39, 488–498.
Saturnino, G.B., Antunes, A., Thielscher, A., 2015. On the importance of electrode parameters for shaping electric field patterns generated by tDCS. Neuroimage 120, 25–35.
Schmaal, L., Hibar, D.P., Sämann, P.G., Hall, G.B., Baune, B.T., Jahanshad, N., Cheung, J.W., van Erp, T.G.M., Bos, D., Ikram, M.A., 2017. Cortical abnormalities in adults and adolescents with major depression based on brain scans from 20 cohorts worldwide in the ENIGMA Major Depressive Disorder Working Group. Mol. Psychiatry 22, 900–909.

Schulze, L., Wheeler, S., McAndrews, M.P., Solomon, C.J., Giacobbe, P., Downar, J., 2016. Cognitive safety of dorsomedial prefrontal repetitive transcranial magnetic stimulation in major depression. Eur. Neuropsychopharmacol. 26, 1213–1226.

Seibt, O., Brunoni, A.R., Huang, Y., Bikson, M., 2015. The pursuit of DLPFC: non-neuronavigated methods to target the left dorsolateral pre-frontal cortex with symmetric bicephalic transcranial direct current stimulation (tDCS). Brain Stimulat. 8, 590–602.

Sheline, Y.I., Price, J.L., Yan, Z., Mintun, M.A., 2010. Resting-state functional MRI in depression unmasks increased connectivity between networks via the dorsal nexus. Proc. Natl. Acad. Sci. USA 107, 11020–11025.

Siegle, G.J., Thompson, W., Carter, C.S., Steinhauer, S.R., Thase, M.E., 2007. Increased amygdala and decreased dorsolateral prefrontal BOLD responses in unipolar depression: related and independent features. Biol. Psychiatry 61, 198–209.

Silvetti, M., Alexander, W., Verguts, T., Brown, J.W., 2014. From conflict management to reward-based decision making: actors and critics in primate medial frontal cortex. Neurosci. Biobehav. Rev. 46, 44–57.

Taylor, T.J., Clark, L., Furey, M.L., Williams, G.B., Sahakian, B.J., Drevets, W.C., 2008. Neural basis of abnormal response to negative feedback in unmedicated mood disorders. NeuroImage 42, 1118–1126.

Thielscher, A., Antunes, A., Saturnino, G.B., 2015. Field modeling for transcranial magnetic stimulation: A useful tool to understand the physiological effects of TMS?, in: IEEE EMBS. pp. 222–225.

Tremblay, S., Lepage, J.F., Latulipe-Loiselle, A., Fregni, F., Pascual-Leone, A., Théoret, H., 2014. The uncertain outcome of prefrontal tDCS. Brain Stimulat. 7, 773–783.

Vehtari, A., Gelman, A., Gabry, J., 2015. Efficient implementation of leave-one-out cross-validation and WAIC for evaluating fitted Bayesian models. ArXiv Prepr. ArXiv150704544.

Villamar, M.F., Volz, M.S., Bikson, M., Datta, A., DaSilva, A.F., Fregni, F., 2013. Technique and considerations in the use of 4x1 ring high-definition transcranial direct current stimulation (HD-tDCS). J. Vis. Exp. JoVE 77, e50309.

Wagner, S., Rampersad, S.M., Aydin, Ü., Vorwerk, J., Oostendorp, T.F., Neuling, T., Herrmann, C.S., Stegeman, D.F., Wolters, C.H., 2014. Investigation of tDCS volume conduction effects in a highly realistic head model. J. Neural Eng. 11, 16002–16015.

Watanabe, S., 2013. A widely applicable Bayesian information criterion. J. Mach. Learn. Res. 14, 867–897.

Wolkenstein, L., Plewnia, C., 2013. Amelioration of cognitive control in depression by transcranial direct current stimulation. Biol. Psychiatry 73, 646–651.

Figures

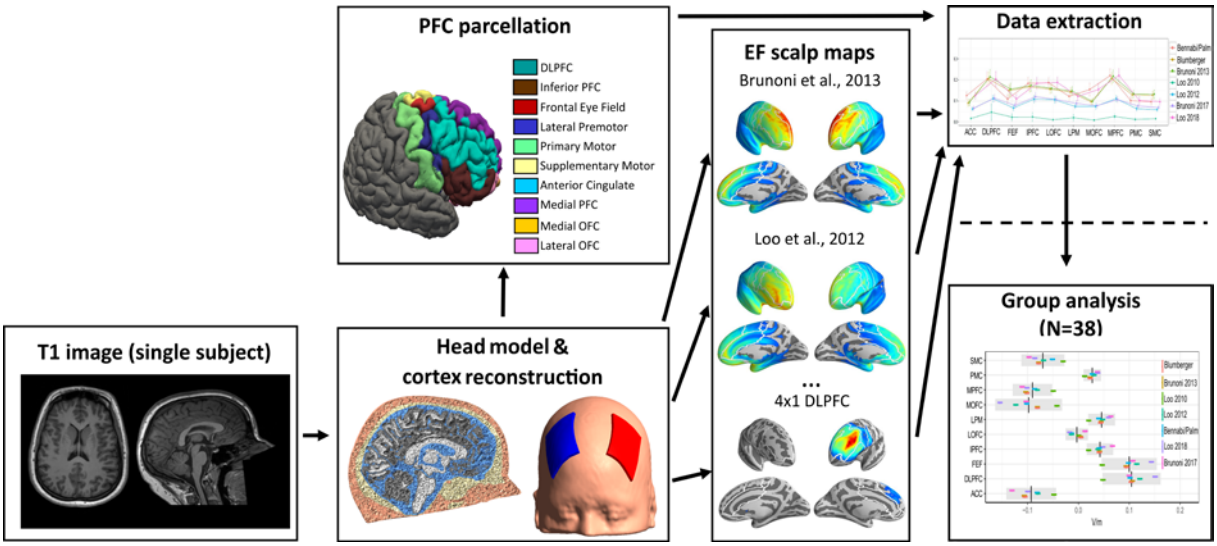

Figure 1. Workflow for data extraction. Abbreviations: DLPFC: dorsolateral prefrontal cortex; EF: electric field; MPFC: medial prefrontal cortex; PFC: prefrontal cortex.

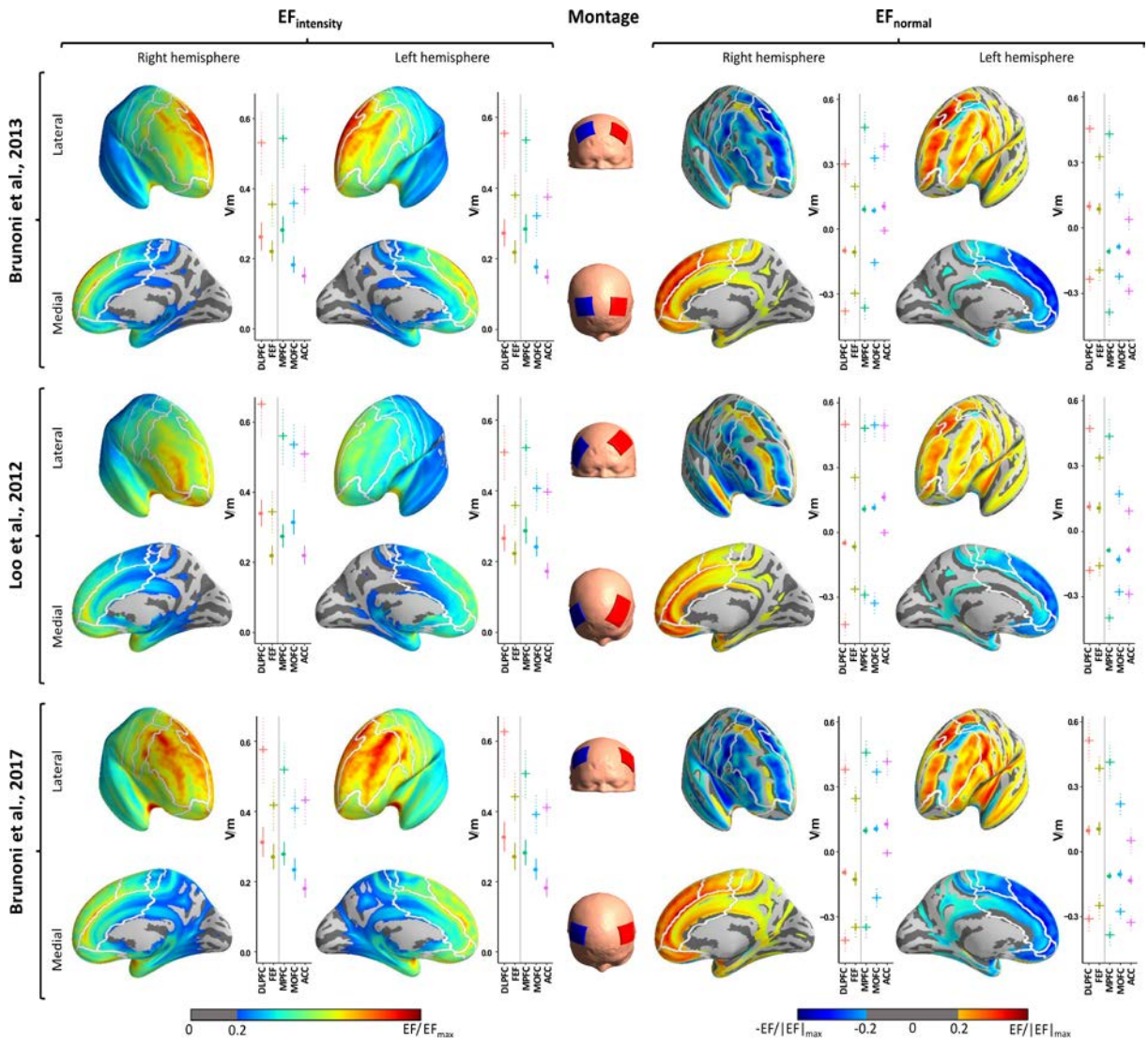

Figure 2. Electric field distributions for the montages by Brunoni et al. (2013), Loo et al. (2012) and Brunoni et al. (2017), shown separately for total electric field strength ($EF_{intensity}$, left) and the electric field component normal to the cortical surface (EF_{normal}, right). Please note that dark blue represents low activity for $EF_{intensity}$, but strong outward-flowing currents for EF_{normal}. Dots and solid lines represent global means and standard deviations (across subjects), whereas plus signs and dotted bars correspond to mean and standard deviations for individual peaks ($EF_{intensity}$: maxima; EF_{normal}: maxima and minima), calculated separately for the five labels of interest (DLPFC: dorsolateral prefrontal cortex; FEF: frontal eye field; MPFC: medial prefrontal cortex; MOFC: medial orbitofrontal cortex; ACC: anterior cingulate

cortex). Scales were normalized to the highest absolute EF value ($|EF|_{max}$) in the entire cortex. Values below 0.2 ($EF_{intensity}$) or between -0.2 and 0.2 (EF_{normal}) are not visualized.

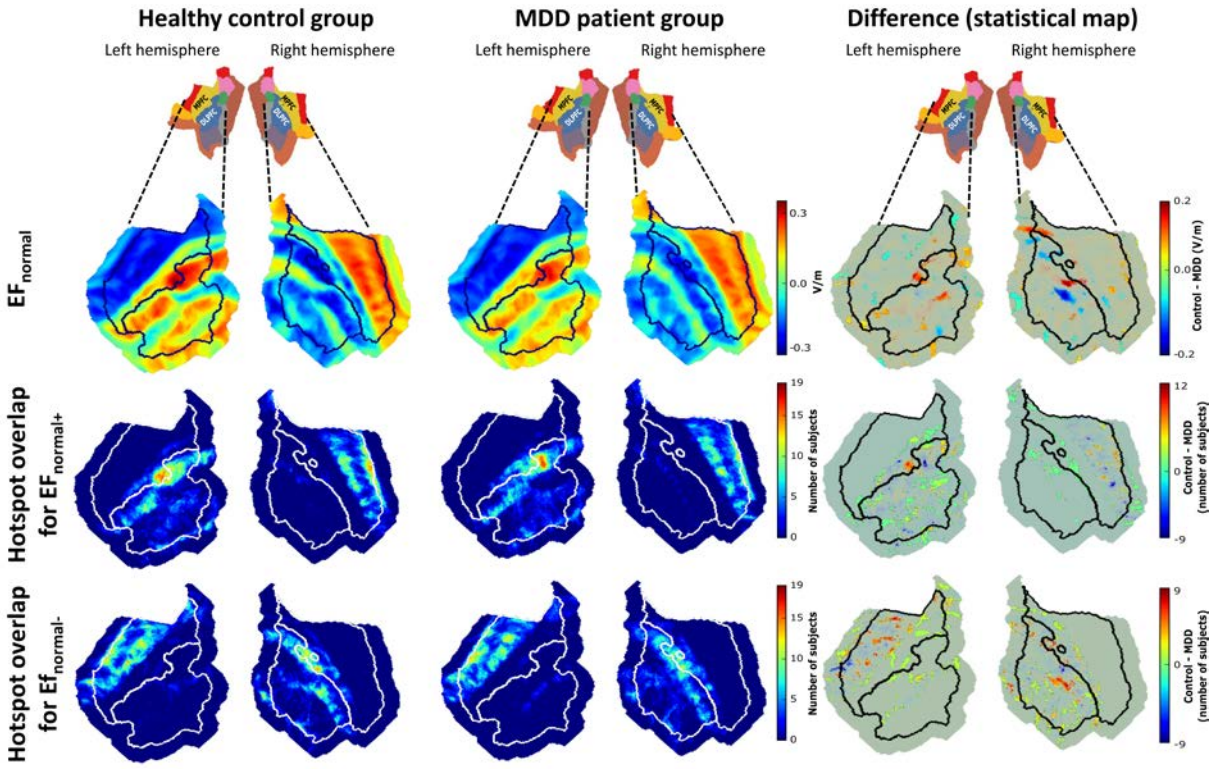

Figure 3. Spatial distribution of currents normal to the cortical surface (EF_{normal}) for the montage by Brunoni et al. (2013) in the flattened bilateral dorsolateral prefrontal cortex (DLPFC) and medial prefrontal cortex (MPFC), plotted separately for healthy participants and MDD patients. Upper row: group mean EF_{normal} values calculated for each node separately. Statistical map shows nodes with control vs. patient EF_{normal} difference values belonging to the top 5% interval with respect to a nonparametric permutation test (with random assignment of participants to 2 groups repeated 1,000 times). Middle and lower rows: spatial overlap of hotspots with EF values in the top 1% (for $EF_{normal+}$) or bottom 1% (for $EF_{normal-}$) range. Statistical maps show nodes with control vs. patient differences that fall within the top or bottom 2.5% intervals with respect to a nonparametric permutation test (1,000 random assignments of participants to 2 groups). Red values indicate nodes with larger degree of hotspot overlap in the control group, whereas blue values depict nodes with substantially more hotspots within patients.

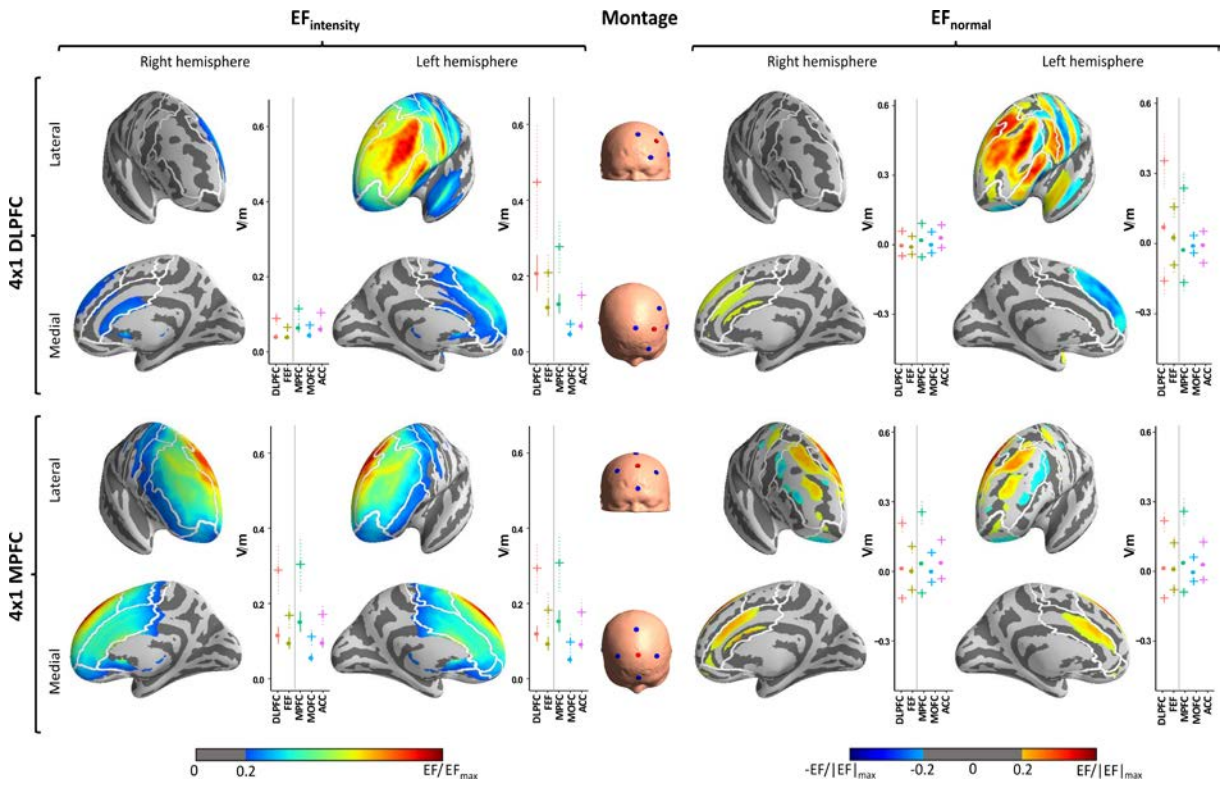

Figure 4. Electric field distributions for the 4x1 montages, shown separately for total electric field strength ($EF_{intensity}$, left) and the electric field component normal to the cortical surface (EF_{normal}, right). Please note that dark blue represents low activity for $EF_{intensity}$, but strong outward-flowing currents for EF_{normal}. Dots and solid lines represent global means and standard deviations (across subjects), whereas plus signs and dotted bars correspond to mean and standard deviations for individual peaks ($EF_{intensity}$: maxima; EF_{normal}: maxima and minima), calculated separately for the five labels of interest (DLPFC: dorsolateral prefrontal cortex; FEF: frontal eye field; MPFC: medial prefrontal cortex; MOFC: medial orbitofrontal cortex; ACC: anterior cingulate cortex). Scales were normalized to the highest absolute EF value ($|EF|_{max}$) in the entire cortex. Values below 0.2 ($EF_{intensity}$) or between -0.2 and 0.2 (EF_{normal}) are not visualized.

Table 1. Main tDCS parameters used for simulation

Parameter	Montage								
	Bennabi et al., 2015 / Palm et al., 2012	**Brunoni et al., 2013**	**Blumberger et al., 2012**	**Loo et al., 2010**	**Loo et al., 2012**	**Brunoni et al., 2017**	**Loo et al., 2018**	**4x 1 DLPFC**	**4x1 MPFC**
Anode position	F3	F3	F3	F3	F3	OLE system (left hemisphere)	F3	F3	Fz
Cathode position	RSO	F4	F4	RSO	F8	OLE system (right hemisphere)	F8	C3, FT7, Fp1, Fz	Fpz, Cz, F3, F4
Electrode size	5 x 7 cm	5 x 5 cm	5 x 7 cm	5 x 7 cm	5 x 7 cm	5 x 5 cm	5 x 7	Diameter: 1.2 cm	Diameter: 1.2 cm
Current intensity	2 mA	2 mA	2 mA	1 mA	2 mA	2 mA	2.5 mA	Anode: 2 mA Cathodes: 0.5 mA	Anode: 2 mA Cathodes: 0.5 mA

OLE: Omni-Lateral Electrode; RSO: right supraorbital

Supplementary Material

Supplementary Methods

Manual procedures

Our data analytic workflow consisted of four manual procedures.

1) As the very first step, we inspected scans of all participants, and manually removed signals corresponding to the MRI marker placed on the forehead of each subject using FreeSurfer.
2) We inspected and manually corrected results of the automated tissue segmentation with FreeSurfer (done by G.Cs., verified by O.P.). Manual corrections were primarily restricted to the skull-CSF boundary, but in some cases also involved the skin-skull interface. The resulting adjusted masks were used for the creation of head models.
3) Following automated PFC parcellation, ACC labels did not consistently encompass the subgenual region (sgACC), an area implicated in MDD (Mayberg et al., 2005). Therefore, we manually adjusted ACC labels for each individual and hemisphere using FreeSurfer to make sure they include the sgACC.
4) In order to define the scalp location of tDCS electrodes individually, we manually defined coordinates corresponding to four reference locations (nasion, inion, left and right pre-auricular points), and run a modified version of a published script (Huang et al., 2013) to obtain the center coordinates of electrodes.

TDCS electrode parameters

For the montage used by Brunoni and colleagues (Brunoni et al., 2013), medial margins of both electrodes were oriented parallel to the midsagittal plane. Orientations of 5 x 7 cm electrodes were adjusted after personal communication with the authors (Bennabi et al., 2015; Blumberger et al., 2012; Loo et al., 2010, 2012; Palm et al., 2012). For the montages used by Bennabi et al. (2015) and Palm et al. (2012), longer edges of both electrodes were oriented perpendicular to the midsagittal plane. For the montage by Blumberger et al. (2012), longer edges of both electrodes were oriented parallel to the midsagittal plane. In the study by Brunoni et al. (2017), electrodes were placed according to the Omni-Lateral Electrode (OLE) System (Brunoni et al., 2017; Seibt et al., 2015). In this protocol, we determined the midpoint between electrodes T7 and T8, and placed a vector at that position, pointing at the inion. Next, we rotated this vector anteriorly by 165° along the midsagittal plane (defined by the nasion-Cz-inion scalp locations) and determined its scalp projection ('frontal midsagittal position'; FMP), which was used for calculating the centers of the tDCS electrodes on the scalp surface. This was done by rotating the vector pointing at FMP along the T7-FMP-T8 plane laterally to the extent that the electrode centers would be positioned 7.5 cm laterally from the FMP along the scalp (assuming that the head has a spherical shape). This way, the distance between the superior margins of both tDCS electrodes was 10 cm (with electrode size of 5x5 cm), as described by the OLE protocol. Electrodes were oriented so that superior electrode margins were perpendicular to the T7-FMP-T8 plane. For the montages used by Loo and colleagues (Loo et al., 2010, 2012, 2018), the longer edge of the anode was oriented towards the nose (with an angle of approximately 45° to the midsagittal plane), whereas the longer edge of the cathode was oriented perpendicular to the line corresponding to the right eyebrow.

For bipolar montages, electrode thickness was always set to 1 mm; sponge pocket thickness was 2.5 mm. We positioned circular connectors (diameter: 0.5 cm) at the middle of

the electrode pads. For the 4x1 montages, electrodes with a diameter of 1.2 cm and thickness of 1 mm were used, with the addition of a gel layer (thickness: 2.5 mm) between the electrode-skin surface.

Data analytic strategy

All reported models were fitted using Hamiltonian Monte-Carlo (HMC) techniques. We sampled from the joint posterior distribution of the parameters given the model using the HMC algorithms implemented in the Stan software (Carpenter et al., 2017; Hoffman and Gelman, 2014). All fits used eight parallel chains, each with a warm-up period of 1,000 samples. Chains were initialized at random values and we sampled 1,000 samples from each of the converged chains. We used no thinning as this was not deemed necessary by visual inspection of the chains and autocorrelation statistics. Resulting samples for each individual variable were visually inspected for convergence to ensure good mixing behaviour. We also applied the Gelman-Rubin diagnostic (Gelman and Rubin, 1992) and ensured that all reported results had $\hat{R} \leq 1.05$.

Supplementary Results

Comparison of spatial focality

As our last analysis, we compared focality-indices (FI) calculated for each bipolar and 4x1 montage separately (Supplementary Figure 5). Given that bipolar montages induced strong EFs in the bilateral MPFC, we compared montages for their ability to selectively induce inward ($EF_{normal+}$) or outward ($EF_{normal-}$) directed fields in either the lDLPFC or the MPFC (FI_{lDLPFC}, FI_{MPFC}, respectively). All bipolar montages exerted similarly selective excitatory effects in the lDLPFC, except for the Loo et al. (2012, 2018) and Brunoni et al. (2018) protocols, yielding lower FI_{lDLPFC} values, probably due to the relatively large number

of hotspots in the lateral aspect of the right hemisphere and inferior regions of the left hemisphere. Additionally, $EF_{normal-}$ values for FI_{lDLPFC} were very close to zero, suggesting the predominance of inward-flowing currents in this region. In accordance with our previous analyses, the FI_{MPFC} was very high in bilateral MPFC, both for anode-like and cathode-like effects, but again, the Loo et al. (2012, 2018) and Brunoni et al. (2018) montages were characterized by lower values.

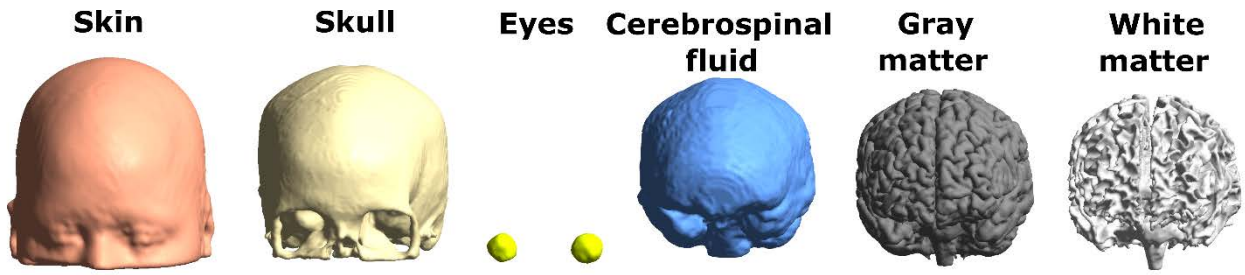

Supplementary Figure 1. The six tissue compartments of the head models.

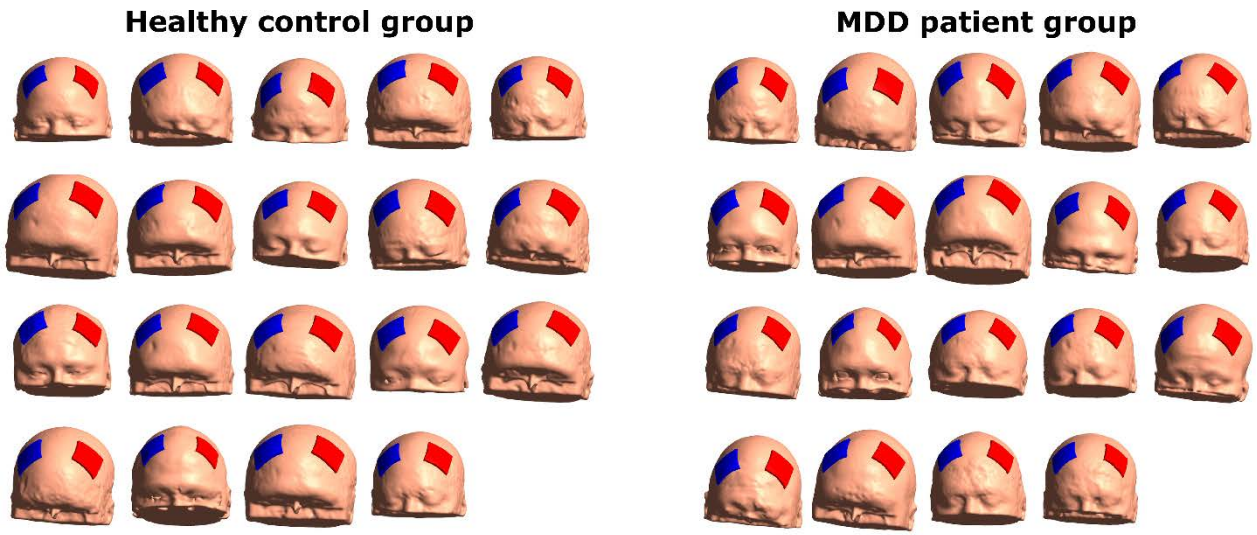

Supplementary Figure 2. The 38 head models with electrodes placed according to the protocol by Brunoni et al. (2013).

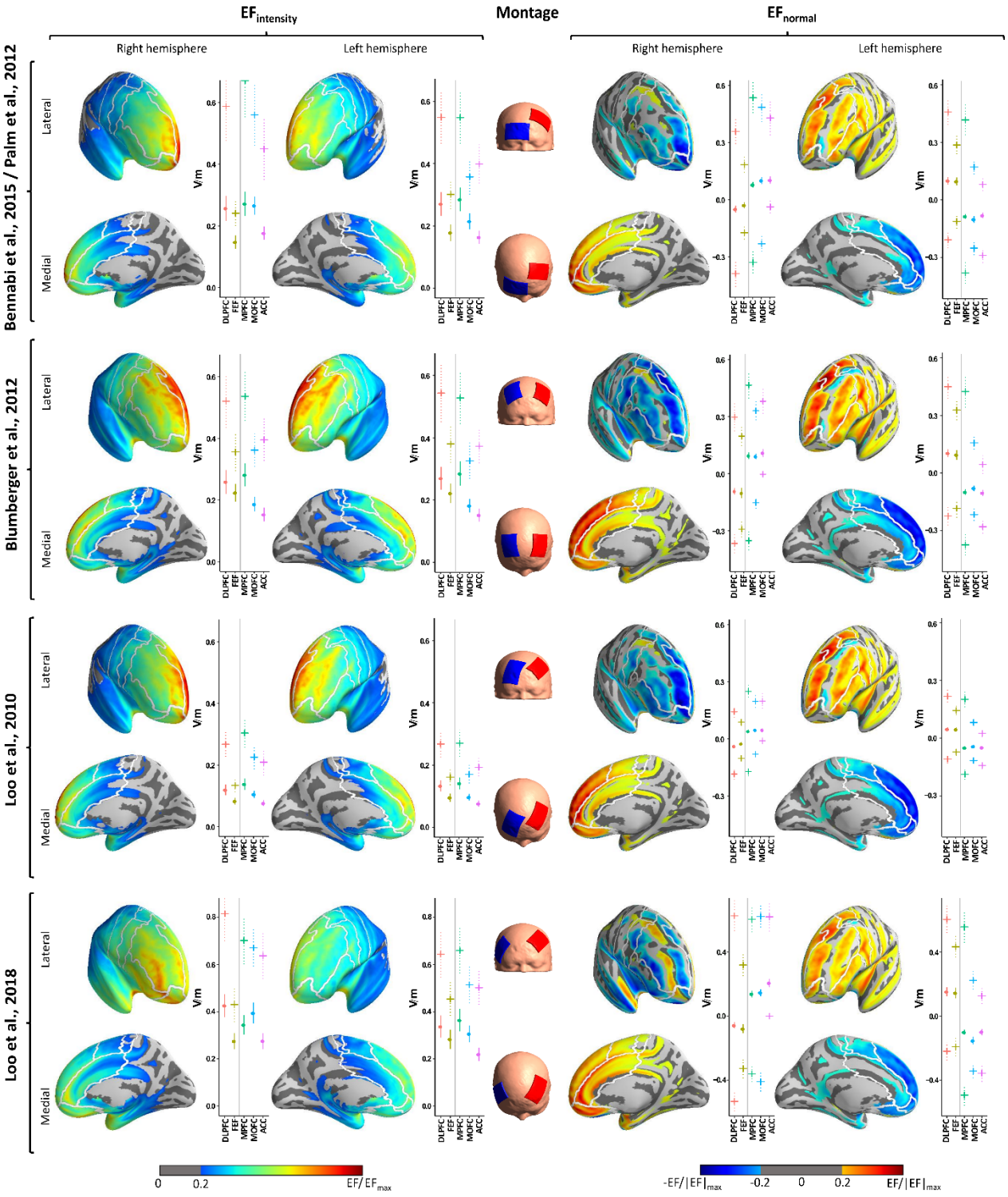

Supplementary Figure 3. Electric field distributions for the Bennabi et al. (2015)/Palm et al. (2012), Blumberger et al. (2012), Loo et al. (2010) and Loo et al. (2018) montages, shown separately for total electric field strength ($EF_{intensity}$, left) and the electric field component normal to the cortical surface (EF_{normal}, right). Please note that dark blue represents low

activity for $EF_{intensity}$, but strong outward-flowing currents for EF_{normal}. Dots and solid lines represent global means and standard deviations (across subjects), whereas plus signs and dotted bars correspond to mean and standard deviations for individual peaks ($EF_{intensity}$: maxima; EF_{normal}: maxima and minima), calculated separately for the five labels of interest (DLPFC: dorsolateral prefrontal cortex; FEF: frontal eye field; MPFC: medial prefrontal cortex; MOFC: medial orbitofrontal cortex; ACC: anterior cingulate cortex). Scales were normalized to the highest absolute EF value ($|EF|_{max}$) in the entire cortex. Values below 0.2 ($EF_{intensity}$) or between -0.2 and 0.2 (EF_{normal}) are not visualized.

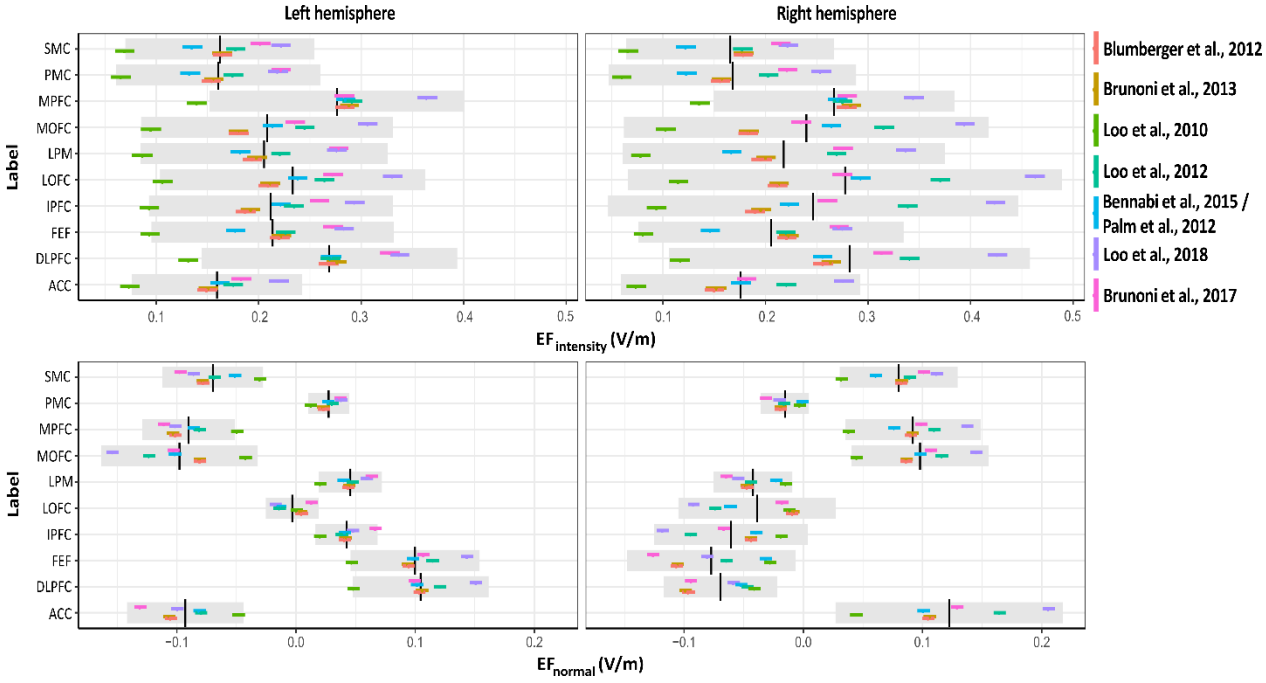

Supplementary Figure 4. Distribution of total electric field strength ($EF_{intensity}$) and currents normal to the cortical surface (EF_{normal}) across the seven bipolar montages, 10 cortical labels (SMC: supplementary motor cortex; PMC: primary motor cortex; MPFC: medial prefrontal cortex; MOFC: medial orbitofrontal cortex; LPM: lateral premotor cortex; LOFC: lateral orbitofrontal cortex; IPFC: inferior prefrontal cortex; FEF: frontal eye field; DLPFC: dorsolateral prefrontal cortex; ACC: anterior cingulate cortex) and two hemispheres. Dots and solid bars represent estimated posterior means and 95% highest-density intervals. Vertical black bars represent means of all montages, gray stripes correspond to 2 * standard deviation.

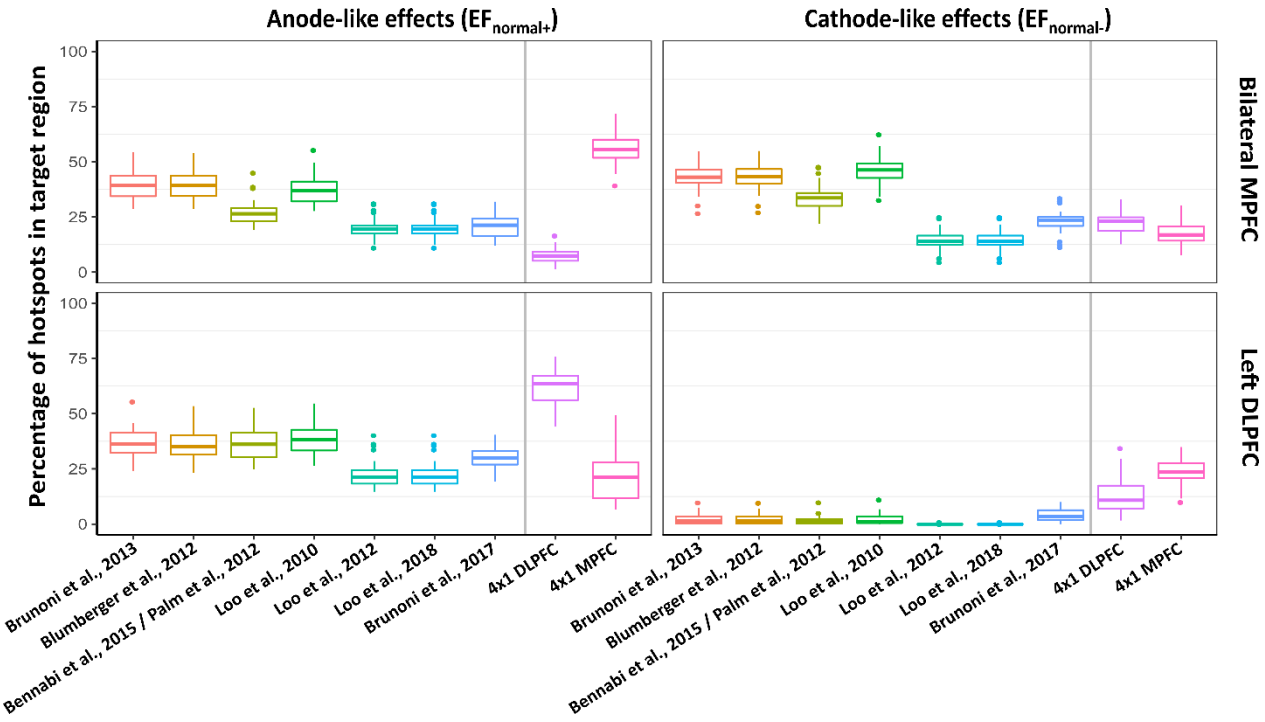

Supplementary Figure 5. Focality-indices (percentage of top 1% nodes in target region) for the bilateral medial prefrontal cortex (MPFC) and left dorsolateral prefrontal cortex (DLPFC), calculated separately for positive and negative EF_{normal} values for all montages. Horizontal lines within boxes represent median values, whereas lower and upper box hinges correspond to the first and third quartiles (25^{th} and 75^{th} percentiles). Lengths of upper/lower whiskers extend to the largest/smallest values that do not exceed 1.5* the inter-quartile range; data beyond the end of whiskers are outliers.

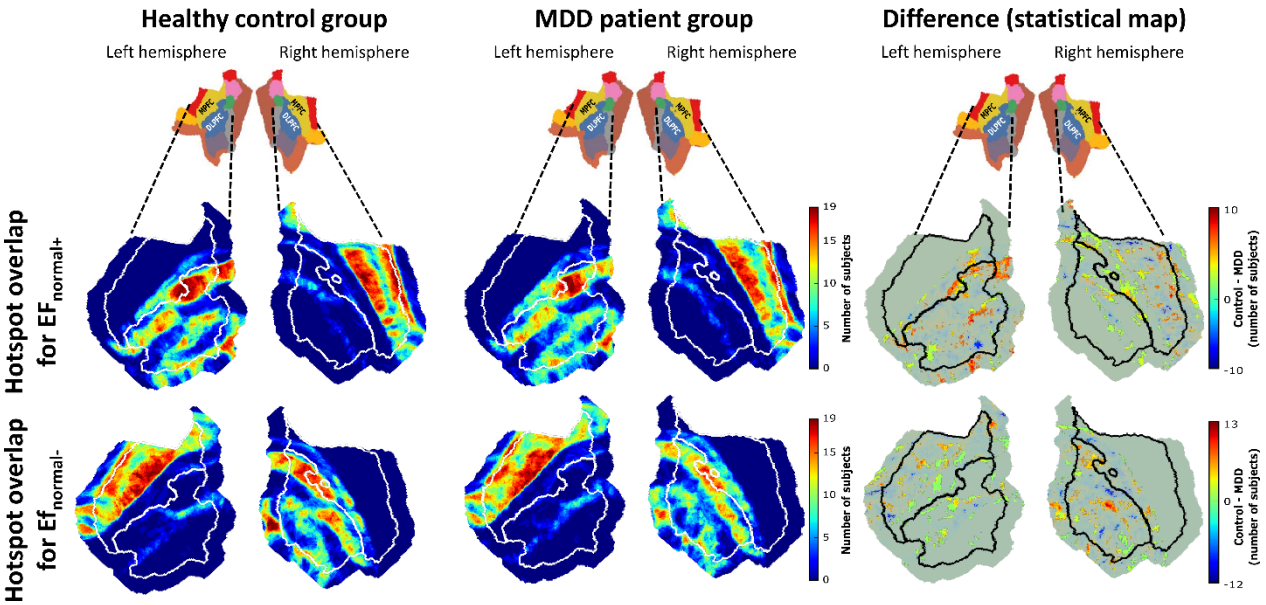

Supplementary Figure 6. Spatial distribution of hotspot (strongest 5% EF_{normal} values) overlap for the Brunoni et al. (2013) montage in the flattened bilateral dorsolateral prefrontal cortex (DLPFC) and medial prefrontal cortex (MPFC), plotted separately for healthy participants and MDD patients (upper row: $EF_{normal+}$; lower row: $EF_{normal-}$). Statistical maps show nodes with control vs. patient differences that fall within the top or bottom 2.5% intervals with respect to a nonparametric permutation test (1,000 random assignments of participants in 2 groups). Red values indicate nodes with larger degree of hotspot overlap in the control group, whereas blue values depict nodes with substantially more hotspots within patients.

Supplementary Table 1. Tissue conductivities used for modeling electric field distributions

Tissue type	**Conductivity (S/m)**
Electrode rubber	0.1
Electrode sponge/gel	1.0
Skin	0.465
Eyeballs	0.5
Skull	0.01
Cerebrospinal fluid	1.654
Gray matter	0.275
White matter	0.126

Supplementary Table 2. Model selection for $EF_{intensity}$ values for the bipolar montages

Model ranking	Free parameter				LOOIC
	Hemisphere	Label	Montage	Group	
1	X	X	X	-	-27,407.3
2	X	X	X	X	-27,260.2
3	-	X	X	-	-23,368.9
4	-	X	X	X	-23,282.0
5	X	-	X	-	-16,502.3
6	X	-	X	X	-16,482.8
7	-	-	X	-	-16,144.1
8	-	-	X	X	-16,139.1
9	X	X	-	-	-13,034.4
10	X	X	-	X	-13,000.2
11	-	X	-	-	-12,922.2
12	-	X	-	X	-12,906.6
13	X	-	-	-	-11,504.4
14	X	-	-	X	-11,502.7
15	-	-	-	X	-11,463.7
16	-	-	-	-	-11,463.4

Supplementary Table 3. Model selection for EF_{normal} values for the bipolar montages

Model ranking	Free parameter				LOOIC
	Hemisphere	Label	Montage	Group	
1	X	X	X	-	-28,513.3
2	X	X	X	X	-28,449.0
3	X	X	-	X	-22,024.0
4	X	X	-	-	-22,009.2
5	-	X	X	-	-11,695.6
6	-	X	-	-	-11,660.8
7	-	X	-	X	-11,641.4
8	X	-	-	-	-11,612.3
9	X	-	-	X	-11,608.5
10	X	-	X	-	-11,601.4
11	-	-	-	-	-11,584.1
12	-	-	-	X	-11,582.3
13	-	-	X	-	-11,582.0
14	X	-	X	X	-11,574.4
15	-	-	X	X	-11,568.1
16	-	X	X	X	-11,555.6

Supplementary Table 4. Model selection for $EF_{intensity}$ values for the 4x1 montages

Model ranking	**Free parameter**				**LOOIC**
	Hemisphere	Label	Montage	Group	
1	X	X	X	-	-12,011.1
2	X	X	X	X	-11,941.5
3	X	X	-	-	-11,227.6
4	X	X	-	X	-11,191.9
5	-	X	X	-	-10,991.1
6	-	X	X	X	-10,953.4
7	-	X	-	-	-10,801.2
8	X	-	X	-	-10,790.6
9	X	-	X	X	-10,785.6
10	-	X	-	X	-10,783.2
11	X	-	-	-	-10,530.1
12	X	-	-	X	-10,528.4
13	-	-	X	-	-10,320.9
14	-	-	-	-	-10,319.0
15	-	-	X	X	-10,318.9
16	-	-	-	X	-10,318.8

Supplementary Table 5. Model selection for EF_{normal} values for the 4x1 montages

Model ranking	Free parameter				LOOIC
	Hemisphere	Label	Montage	Group	
1	X	X	X	-	-10,732.4
2	X	X	X	X	-10,697.0
3	X	X	-	-	-8,796.3
4	X	X	-	X	-8,767.1
5	-	X	X	-	-8,637.1
6	-	X	X	X	-8,602.1
7	-	X	-	-	-8,241.7
8	-	X	-	X	-8,225.2
9	-	-	X	-	-7,519.5
10	-	-	-	-	-7,518.1
11	X	-	-	-	-7,517.2
12	X	-	X	-	-7,516.6
13	-	-	-	X	-7,516.5
14	-	-	X	X	-7,515.7
15	X	-	-	X	-7,513.9
16	X	-	X	X	-7,509.2

Supplementary References

Bennabi, D., Nicolier, M., Monnin, J., Tio, G., Pazart, L., Vandel, P., Haffen, E., 2015. Pilot study of feasibility of the effect of treatment with tDCS in patients suffering from treatment-resistant depression treated with escitalopram. Clin. Neurophysiol. 126, 1185–1189.

Blumberger, D.M., Tran, L.C., Fitzgerald, P.B., Hoy, K.E., Daskalakis, Z.J., 2012. A randomized double-blind sham-controlled study of transcranial direct current stimulation for treatment-resistant major depression. Front. Psychiatry 3, 74.

Brunoni, A.R., Moffa, A.H., Sampaio-Junior, B., Borrione, L., Moreno, M.L., Fernandes, R.A., Veronezi, B.P., Nogueira, B.S., Aparicio, L.V.M., Razza, L.B., 2017. Trial of Electrical Direct-Current Therapy versus Escitalopram for Depression. N. Engl. J. Med. 376, 2523–2533.

Brunoni, A.R., Valiengo, L., Baccaro, A., Zanão, T.A., de Oliveira, J.F., Goulart, A., Boggio, P.S., Lotufo, P.A., Benseñor, I.M., Fregni, F., 2013. The sertraline vs. electrical current therapy for treating depression clinical study: results from a factorial, randomized, controlled trial. JAMA Psychiatry 70, 383–391.

Carpenter, B., Gelman, A., Hoffman, M.D., Lee, D., Goodrich, B., Betancourt, M., Brubaker, M., Guo, J., Li, P., Riddell, A., 2017. Stan: A Probabilistic Programming Language. J. Stat. Softw. 76, 1–32.

Gelman, A., Rubin, D.B., 1992. Inference from iterative simulation using multiple sequences. Stat. Sci. 457–472.

Hoffman, M.D., Gelman, A., 2014. The No-U-Turn Sampler: Adaptively Setting Path Lengths in Hamiltonian Monte Carlo. J. Mach. Learn. Res. 15, 1351–1381.

Huang, Y., Dmochowski, J.P., Su, Y., Datta, A., Rorden, C., Parra, L.C., 2013. Automated MRI segmentation for individualized modeling of current flow in the human head. J. Neural Eng. 10, 066004–066004.

Loo, C.K., Alonzo, A., Martin, D., Mitchell, P.B., Galvez, V., Sachdev, P., 2012. Transcranial direct current stimulation for depression: 3-week, randomised, sham-controlled trial. Br. J. Psychiatry 200, 52–59.

Loo, C.K., Husain, M.M., McDonald, W.M., Aaronson, S., O'Reardon, J.P., Alonzo, A., Weickert, C.S., Martin, D.M., McClintock, S.M., Mohan, A., 2018. International randomized-controlled trial of transcranial Direct Current Stimulation in depression. Brain Stimulat. 11, 125–133.

Loo, C.K., Sachdev, P., Martin, D., Pigot, M., Alonzo, A., Malhi, G.S., Lagopoulos, J., Mitchell, P., 2010. A double-blind, sham-controlled trial of transcranial direct current stimulation for the treatment of depression. Int. J. Neuropsychopharmacol. 13, 61–69.

Mayberg, H.S., Lozano, A.M., Voon, V., McNeely, H.E., Seminowicz, D., Hamani, C., Schwalb, J.M., Kennedy, S.H., 2005. Deep brain stimulation for treatment-resistant depression. Neuron 45, 651–660.

Palm, U., Schiller, C., Fintescu, Z., Obermeier, M., Keeser, D., Reisinger, E., Pogarell, O., Nitsche, M.A., Möller, H.J., Padberg, F., 2012. Transcranial direct current stimulation in treatment resistant depression: a randomized double-blind, placebo-controlled study. Brain Stimulat. 5, 242–251.

Seibt, O., Brunoni, A.R., Huang, Y., Bikson, M., 2015. The pursuit of DLPFC: non-neuronavigated methods to target the left dorsolateral pre-frontal cortex with symmetric bicephalic transcranial direct current stimulation (tDCS). Brain Stimulat. 8, 590–602.